

# UC San Diego

## UC San Diego Electronic Theses and Dissertations

### Title

Topics in Khovanov homology

### Permalink

<https://escholarship.org/uc/item/4sq5g6ct>

### Author

Wilson, Benjamin Edward

### Publication Date

2012

Peer reviewed|Thesis/dissertation

UNIVERSITY OF CALIFORNIA, SAN DIEGO

**Topics in Khovanov Homology**

A dissertation submitted in partial satisfaction of the  
requirements for the degree  
Doctor of Philosophy

in

Mathematics

by

Benjamin Wilson

Committee in charge:

Professor Justin Roberts, Chair  
Professor Ken Intriligator  
Professor David Meyer  
Professor Dan Rogalski  
Professor Vivek Sharma

2012

Copyright  
Benjamin Wilson, 2012  
All rights reserved.

The dissertation of Benjamin Wilson is approved,  
and it is acceptable in quality and form for publi-  
cation on microfilm:

---

---

---

---

---

Chair

University of California, San Diego

2012

## DEDICATION

To my family, Ed, Lynn, Kim, Pandora and J-ray.

## EPIGRAPH

*A man who carries a cat by the tail  
learns something he can learn no other way.*

—Mark Twain

## TABLE OF CONTENTS

Signature Page . . . . .	iii
Dedication . . . . .	iv
Epigraph . . . . .	v
Table of Contents . . . . .	vi
List of Figures . . . . .	viii
List of Tables . . . . .	ix
Acknowledgements . . . . .	x
Vita and Publications . . . . .	xi
Abstract . . . . .	xi
Chapter 1 Introduction . . . . .	1
1.1 A Brief History of Link Invariants . . . . .	1
1.2 Link Homologies . . . . .	2
1.3 Organization and Summary of Results . . . . .	3
Chapter 2 Preliminaries . . . . .	5
2.1 Knots and Links . . . . .	5
2.2 Braids . . . . .	7
2.3 Torus Links . . . . .	8
2.4 Jones Polynomial . . . . .	9
Chapter 3 Khovanov and Lee Homology . . . . .	11
3.1 Graded Modules . . . . .	11
3.2 Khovanov’s Construction . . . . .	12
3.3 Properties of Khovanov Homology . . . . .	15
3.4 Lee Homology . . . . .	18
3.5 A Categorical Formulation Encapsulating Khovanov and Lee Homology . . . . .	20
Chapter 4 Bounds on Rasmussen’s Invariant . . . . .	25
4.1 Lee Homology and Oriented Resolutions . . . . .	25
4.2 Construction of the chain maps . . . . .	31
4.3 Bounds on Rasmussen’s Invariant . . . . .	38
4.4 Representative Cycles . . . . .	41
Chapter 5 Positive Braids and Thickness . . . . .	45
5.1 Garside Powers and Thickness . . . . .	45

Chapter 6 Injectivity of Homology of Certain Links . . . . .	53
6.1 The Reidemeister Invariance Maps . . . . .	53
6.2 Injectivity Result . . . . .	57
6.3 Examples and Ribbon Knot Construction . . . . .	60
6.4 Future Work . . . . .	64
Bibliography . . . . .	68



LIST OF FIGURES

Figure 2.1: Reidemeister Moves . . . . . 6  
 Figure 2.2: The Kauffman state-sum calculation of the trefoil knot . . . . . 10  
 Figure 3.1: Chain Complex for the Trefoil Knot . . . . . 14  
 Figure 3.2:  $Kh(\text{Trefoil}) = q^1 + q^3 + t^2q^5 + t^3q^9$  . . . . . 16  
 Figure 3.3:  $Kh(9_{42}) = t^{-4}q^{-7} + t^{-3}q^{-3} + t^{-2}q^{-2} + t^{-1}q^{-1} + t^{-1}q^1 + q^{-1} + q^1 + q^3 + t^1q^3 + t^2q^7$  . . . . . 17  
 Figure 3.4: The spectral sequence cancellation of  $\mathcal{H}(9_{42})$  . . . . . 20  
 Figure 4.1: The oriented resolution of the knot  $9_{40}$  . . . . . 26  
 Figure 4.2: The composition  $\varphi'_A \circ \varphi_A$  . . . . . 30  
 Figure 4.3: The Seifert graph of the knot  $9_{40}$  . . . . . 31  
 Figure 4.4: Associated Seifert graphs of the knot  $9_{40}$  . . . . . 32  
 Figure 4.5: The resulting chain map  $I$  for the knot  $4_1$  . . . . . 34  
 Figure 4.6: A homogeneous diagram of the knot  $9_{43}$  . . . . . 41  
 Figure 6.1: Constructing the  $6_1$  knot with ribbon moves . . . . . 58  
 Figure 6.2: The diagram  $D_1$  . . . . . 59  
 Figure 6.3: The resulting chain map  $C(D_1) \rightarrow C(D_1)$  . . . . . 60  
 Figure 6.4: Two stage ribbon knot construction . . . . . 61  
 Figure 6.5: Construction of the knot  $10_{147}$  from the trefoil knot . . . . . 62  
 Figure 6.6: Construction of the knot  $10_{99}$  . . . . . 63  
 Figure 6.7: Construction of a ribbon knot using three minima and two saddles 64  
 Figure 6.8: Ribbon presentations of the knots  $10_3$  and  $10_{35}$  . . . . . 65

LIST OF TABLES

Table 5.1:	Thickness of Garside Braid ( $\Delta_n$ ) Closures . . . . .	51
Table 5.2:	Thickness of squares of Garside Braid ( $\Delta_n^2$ ) Closures . . . . .	51
Table 6.1:	Total ranks of ribbon knots of fewer than 11 crossings . . . . .	66

## ACKNOWLEDGEMENTS

Thanks to Justin Roberts for his patience and guidance. Thanks to David Meyer for his support throughout my time at UCSD. Thanks to Jim Lin and the department for the opportunity to be the Senior Teaching Assistant.

## VITA

- 2004 B. S. in Mathematics, University of Nevada, Reno
- 2006 M. S. in Mathematics, University of Nevada, Reno
- 2012 Ph. D. in Mathematics, University of California, San Diego

# ABSTRACT OF THE DISSERTATION

## **Topics in Khovanov Homology**

by

Benjamin Wilson

Doctor of Philosophy in Mathematics

University of California San Diego, 2012

Professor Justin Roberts, Chair

In this dissertation we work with Khovanov homology and its variants. Khovanov homology is a “categorification” of the Jones polynomial. It consists of graded chain complexes which, up to chain homotopy, are link invariants, and whose graded Euler characteristic is equal to the Jones polynomial of the link. Rasmussen’s invariant gives a bound on the smooth 4-ball genus of a knot. We construct bounds on Rasmussen’s invariant which are easily computable from any diagram. Using this construction, one also obtains representatives for the homology classes of the Lee homology of the knot. These bounds are sharp precisely for homogeneous knots, a class of knots containing both alternating knots and positive knots. We prove that a class of braid-positive links, more general than torus links, are Khovanov thick. From this observation we get infinite families of prime knots all of which are Khovanov thick. This is further evidence toward Khovanov’s conjecture that all braid positive knots other than the  $T(2, 2k + 1)$  torus knots are thick. We provide a technique for creating cobordisms between knots which result in injections at the homological level. The technique is applied and studied in the case of ribbon knots.

# Chapter 1

## Introduction

One of the latest developments in knot theory is the construction of “categorified” link invariants, initiated by Mikhail Khovanov in his paper “A Categorification of the Jones Polynomial”. This construction gives new tools for attacking and solving various problems in low dimensional topology.

### 1.1 A Brief History of Link Invariants

Mathematical properties of knots - circles smoothly embedded in 3-space - have been studied for a long time. Carl Gauss discovered the link integral for computing the linking number of two knots in the early eighteenth hundreds. A convenient way of studying links is through planar projections called diagrams, projecting the link down to two dimensions. Knots and links are studied up to isotopy, and hence invariants (functions which agree on all presentations of a given link) are needed to distinguish links.

The tabulation of knots began in the nineteenth century as well with Peter Tait. In the early twentieth century, topologists J.W. Alexander and Kurt Reidemeister began studying knots. This led to the development of the Reidemeister moves. These are a set of moves on planar diagrams of links. Two diagrams represent the same link if and only if they are related by a series of Reidemeister moves. This also led to the development of the the Alexander polynomial, a polynomial invariant of links. This invariant was fairly strong at distinguishing knots and was originally defined geometrically. In the 1970s, Conway showed that this invariant could be described

combinatorially. He also showed that the invariant satisfied a skein relation, which means that diagrams which differ locally (in a specific way) have related invariants.

In 1984, Vaughn Jones discovered what is now known as the Jones polynomial. The recursively defined formula was fairly computable and proved to be a very strong invariant of knots. Very few knots with small crossing numbers exhibited equal Jones polynomials. This discovery led to the introduction of many other polynomial invariants, such as the HOMFLYPT polynomial, and the Kauffman bracket, one of the key ingredients being the idea of a skein relation. Edward Witten proposed new framework for the Jones polynomial with ideas from physics which implied related invariants for three manifolds. Simultaneously, the quantum invariants by Witten, Reshetikhin, and Turaev were developed.

The latest development in the field of link invariants, discovered around the year 2000, are the Khovanov and knot Floer homologies. These are generalizations of the Jones and Alexander polynomial. We describe them in more detail in the next section.

## 1.2 Link Homologies

In his 2000 paper [Kho00], Mikhail Khovanov developed a new perspective on link invariants. He created a “categorified” version of the Jones polynomial. In this case, this means he developed a chain complex related to a link whose graded Euler characteristic is equal to the Jones polynomial of that link. This development is analogous to the relationship between the ranks of simplicial homology groups and Betti numbers. In that case, the Euler characteristic of the simplicial complex is given by either the alternating sum of the Betti numbers or the alternating sum of the ranks of the homology groups.

The categorification is achieved by taking a modified version of Kauffman’s state-sum formula and building a chain complex whose pieces match those of the terms in the sum. It has been shown that this construction is functorial, meaning that maps between links give rise to maps between their homologies in a well defined way. This was first shown, up to sign, by Jacobsson [Jac04]. The sign ambiguity was later removed by Clark, Morrison, and Walker [CMW09]. We will investigate some of these cobordisms in later chapters. The construction given by Khovanov is also a strictly

stronger invariant than the Jones polynomial. There are knots ( $5_1$  and  $10_{132}$ ) which have the same Jones polynomial, but different Khovanov homology.

Khovanov homology has allowed for proofs of theorems that were previously only possibly via gauge theory. Jacob Rasmussen [Ras04] gave a relatively short combinatorial proof of the Milnor Conjecture, which states that the slice genus of the  $(p, q)$  torus knot is  $(p - 1)(q - 1)$ . These combinatorial type proofs and ultimate computability of the invariant have given rise to many of the current open questions regarding Khovanov homology.

The Khovanov complex has a nice combinatorial description and was shown to be very computable [BN07]. Many conjectures were based on these early computations, some of which are listed in [Kho03]. One of the conjectures, is about the “thickness” of Khovanov’s homology. Due to the work of E.S. Lee, alternating links are shown to have “thin” homology. We focus our attention on positive braids, which are very different from alternating knots and are conjectured to have “thick” Khovanov homology.

### 1.3 Organization and Summary of Results

This dissertation is organized as follows. In chapter 2, we describe the basics of knots, links, braids and the Jones polynomial.

In chapter 3, we describe the construction of Khovanov homology and its variants. We also describe the properties enjoyed by Khovanov homology, which will be readily used in the following chapters.

In chapter 4, we develop a method of bounding the  $s$ -invariant. This method not only gives bounds on the  $s$ -invariant, but also gives the homological representatives in the expected quantum grading. This means that, since the  $s$  invariant of a knot is a lower bound for the smooth slice genus of a knot, we can determine a lower bound on the smooth slice genus of a knot simply by combinatorial methods using any one of its diagrams.

In chapter 5, we develop a method providing more evidence toward a conjecture of Khovanov regarding the thickness of positive braid closures. We show that, when written in a certain normal form, many positive braids are Khovanov thick.



In chapter 6, we investigate the effect of cobordisms of small genus on the homology of links. If two links are related by a specific set of “finger” moves and ultimately a merging of components, then their homologies are related.

# Chapter 2

## Preliminaries

### 2.1 Knots and Links

By a knot we mean a smooth embedding of  $S^1$  into  $\mathbb{R}^3$  (or  $S^3$ ). By a link we mean a disjoint collection of knots. We will denote the number of components of a link  $L$  by  $|L|$ . We will consider links only up to isotopy, where one link can be continuously deformed to another. Every knot that can be isotoped to the standard circle will be referred to as the unknot. By a link invariant, we mean any function on the set of links which gives the same value on all links in an isotopy class.

To every link we can associate a diagram by taking a regular projection onto  $\mathbb{R}^2$ . Such a diagram has only finitely many double points and at each point retains information about crossings, distinguishing the over-strand from the under-strand. Due to the work of Reidemeister, two diagrams are said to represent isotopic links if and only if they are related by a series of Reidemeister moves. Two diagrams are related by a Reidemeister move if they differ locally by one of the moves in figure 2.1.

Thus a function defined on diagrams is a link invariant if and only if it is invariant under Reidemeister moves. This allows us to study invariants of links by studying their diagrams. We can associate an orientation to a knot and a knot diagram by indicating which direction the knot is traversed. A link is oriented by choosing an orientation for each component. For an oriented link diagram, each crossing will resemble one of the following:

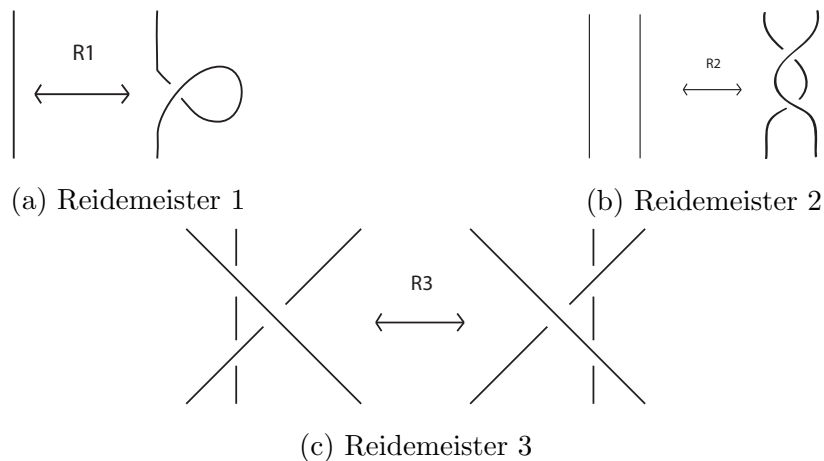
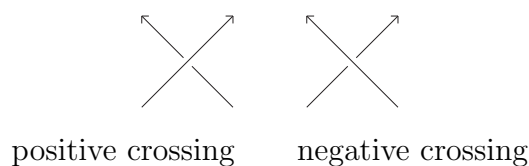
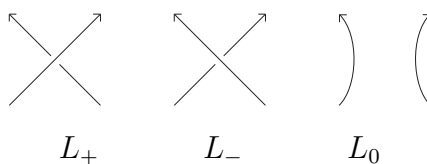


Figure 2.1: Reidemeister Moves



For a link diagram  $D$ , we let  $n_+(D)$  ( $n_-(D)$ ) represent the number of positive (negative) crossings. We denote the writhe of diagram  $w(D) = n_+(D) - n_-(D)$ . We say that a diagram is positive if all crossings present are positive crossings. We will discuss invariants satisfying a skein relation involving the following local pictures



The pictures are meant to represent three link diagrams who differ only in a small neighborhood.  $L_+$  and  $L_-$  represent the diagram with a positive and negative crossing, respectively and  $L_0$  is known as the oriented resolution of the crossing.

A link diagram is said to be alternating if, when one follows the strands of each component, the strand alternates between overstrand and understrand at consecutive crossings. A link is said to be alternating if it has at least one alternating diagram. A knot diagram is positive if all of the crossings in the diagram are positive. A knot is called positive if it has a positive diagram.

The connected sum of two oriented knots  $K_1$  and  $K_2$ , denoted  $K_1 \# K_2$ , is the knot obtained by the following procedure. Take disjoint projections of each knot in the plane. Find a rectangle in the plane whose boundary has four components,

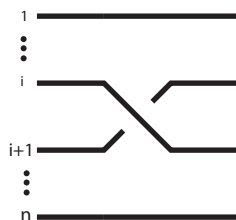
two disjoint from the knots and one component on each knot. Remove the boundary components of the rectangle which intersect the knots and replace with the two boundary components which do not intersect the knot. The result will be a diagram representing a single knot. To perform a connected sum of links, one may perform a similar procedure by first selecting the component of each link which is to be joined. The resulting connected sum of  $L_1$  and  $L_2$  will have  $|L_1| + |L_2| - 1$  components. A knot is said to be prime if it is not the connected sum of two nontrivial knots.

## 2.2 Braids

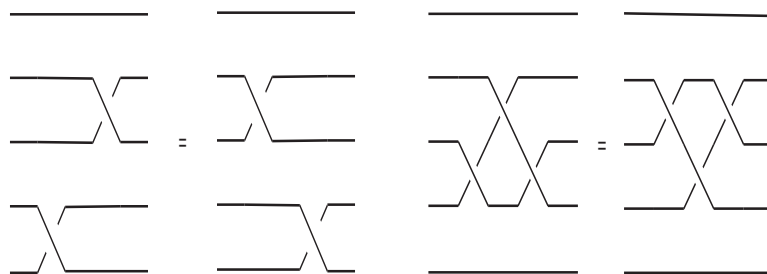
The braid groups were introduced by E. Artin in his 1925 paper. They give us an alternate way of describing links. We now provide a description of Artin's braid group. For each  $n \in \mathbb{Z}$ , we have a group

$$B_n = \{\sigma_1, \dots, \sigma_{n-1} \mid \sigma_i \sigma_j = \sigma_j \sigma_i \text{ if } |i - j| > 1, \quad \sigma_i \sigma_j \sigma_i = \sigma_j \sigma_i \sigma_j \text{ if } |i - j| \leq 1\}$$

called the braid group on  $n$  strands. These relations are most easily seen using diagrams. The generators  $\sigma_i$  are strand crossings of the form



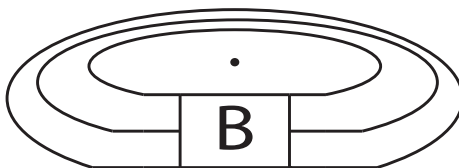
The relations in the braid group are



A braid is said to be positive if it can be written such that the exponents of each generator have the same sign. We use  $B_n^+$  to denote the subsemigroup of  $B_n$  consisting of such braids.

Two braids  $b_1, b_2 \in B_n$  are said to be equivalent if  $\tau^{-1} b_1 \tau = b_2$  for some braid  $\tau \in B_n$ . We can close a braid to give a link by connecting corresponding ends in pairs

as follows



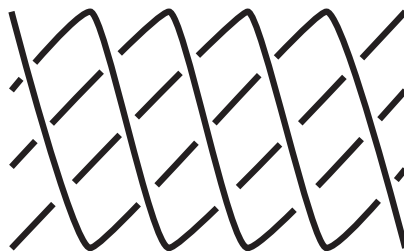
**Proposition 2.2.1** (Alexander). *Every link can be obtained as the closure of a braid.*

Conjugate braids give isotopic links when closed. A more general result of Markov gives a precise condition on when two braid closures represent the same link. A Markov stabilization  $M^\pm : B_n \rightarrow B_{n+1}$  is a transformation given by  $M^+(b) = b\sigma_n$  and  $M^-(b) = b\sigma_n^{-1}$ .

**Theorem 2.2.2.** (Markov) *Two braids represent isotopic links if and only if one can pass from one to the other by using conjugations in the braid group, Markov stabilizations and their inverses.*

## 2.3 Torus Links

In chapter 5 we make reference to a special kind of link, called a torus link. Such links are specified by pairs of integers  $p$  and  $q$ . The torus link  $T_{p,q}$  is link which winds around an unkotted torus in  $\mathbb{R}^3$   $p$  times longitudinally and  $q$  times meridionally. Such links can also be given a description via braids. The  $T_{p,q}$  torus link can be obtained as the closure of the braid on  $p$  strands given by  $(\sigma_1 \cdots \sigma_{p-1})^q$ . Below is a picture of the braid representing the  $T_{4,5}$  torus knot, with 4 strands and 5 full crossings.



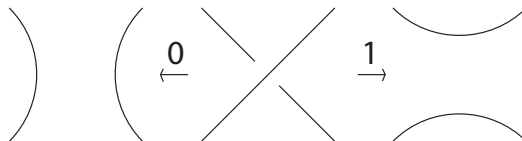
The torus link  $T_{p,q}$  will be a knot if  $p$  and  $q$  are coprime. The torus link is trivial if and only if  $p = \pm 1$  or  $q = \pm 1$ . For any  $p$  and  $q$ , the torus links  $T_{p,q}$  and  $T_{q,p}$  are isotopic. This is not so easily seen in the braid presentation, (they don't even have the same number of crossings!), but is straightforward from the torus embedding definition.

## 2.4 Jones Polynomial

To distinguish links, one typically uses link invariants. These are often computed using a diagram of the link. The Jones polynomial is a Laurent polynomial in the variable  $t^{1/2}$ . We denote the Jones polynomial of a link  $L$  by  $V_L(t)$ . The most elementary way to compute the Jones polynomial is by skein theory. One uses the normalization  $V_U(t) = 1$  for the unknot and recursively uses the following skein relation to obtain a polynomial in  $t^{1/2}$ .

$$t^{-1}V_{L_+} - tV_{L_-} = (t^{1/2} - t^{-1/2})V_{L_0}$$

Another, more tractable approach was offered by Kauffman. He introduced the bracket operation for diagrams which gives a state-sum model for computing the Jones polynomial. The computation is remarkably straightforward and computable. These relations were originally defined in terms of the variable  $t^{1/2}$ , but we use a different variable  $q^2 = t$  and a renormalization based on  $V_U(q) = (q + q^{-1})$  for the unknot. To describe the state-sum formula, we need to introduce some notation. Let  $D$  be a link diagram. For a crossing, there are two possible “smoothings” defined according to the following picture



One can perform a smoothing at each crossing in  $D$ . The result of smoothing each crossing, called a state, will be a set of circles in the plane. We can encode states combinatorially by choosing a 0 or 1 resolution for each crossing in the diagram. Thus, if  $D$  has  $n$  crossings, each length  $n$  binary string  $s \in \{0, 1\}^n$  corresponds to a specific state for the given diagram. To each such string, we assign the following variables. Let  $r(s)$  be the number of 1s in  $s$  and let  $k(s)$  denote the number of circles in the corresponding resolution of  $D$ . To each such state, we assign the value  $q^{r(s)}(q + q^{-1})^{k(s)}$ . The state-sum is as follows

$$\langle D \rangle = \sum_{\text{states } s} (-1)^{r(s)} q^{r(s)} (q + q^{-1})^{k(s)}$$

An alternative definition of the Kauffman bracket is as follows. We can recursively define the bracket with the relations

$$\langle \diagdown \diagup \rangle = \langle \rangle \langle \rangle - q \langle \cup \rangle \quad \langle \bigcirc D \rangle = (q + q^{-1}) \langle D \rangle$$

$$\langle \emptyset \rangle = 1$$

With these definitions we assume that the diagrams look the same except for where the local relation occurs. From these properties we can see that the Kauffman bracket is invariant under Reidemeister 3 moves, but has the following relation with Reidemeister 1 and 2 moves.

$$\langle \text{twist} \rangle = q^{-1} \langle \rangle \quad \langle \text{crossing} \rangle = -q^2 \langle \rangle \quad \langle \text{link} \rangle = -q^{-1} \langle \rangle \langle \rangle$$

From these relations, we can see that a correction term is needed to make the bracket an actual link invariant. That renormalization factor is  $(-1)^{n-} q^{n+ - 2n-}$ . With this correction, the Jones polynomial is then related to the bracket in the following way

$$V_L(q) = (-1)^{n-} q^{n+ - 2n-} \langle D \rangle$$

We now include a graphic for the calculation of the Kauffman bracket for the trefoil knot, presented as the closure of a positive braid. The corresponding factors from each of states is represented at the bottom of the diagram.

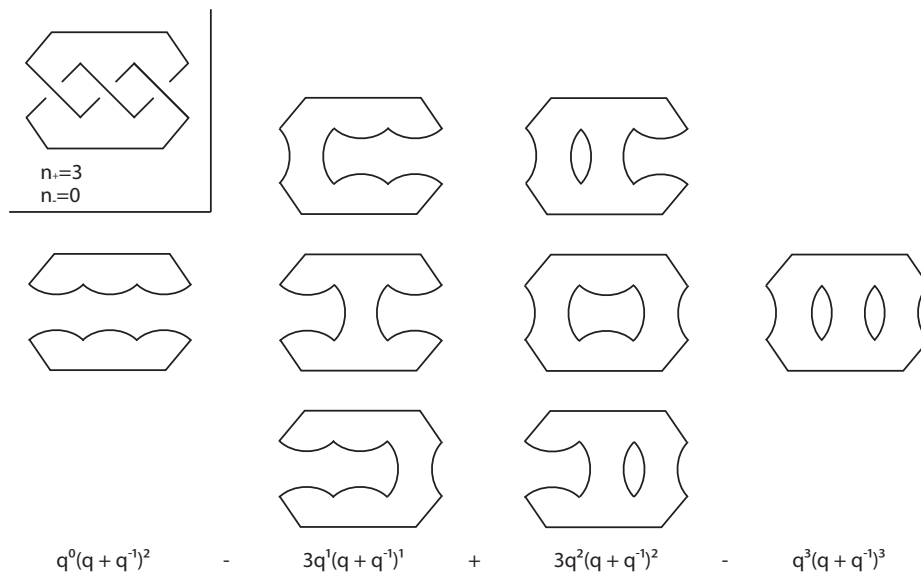


Figure 2.2: The Kauffman state-sum calculation of the trefoil knot

Using this calculation and the writhe corrected formula we obtain  $V_{\text{trefoil}}(q) = q^2 + q^6 - q^8$ .

# Chapter 3

## Khovanov and Lee Homology

Khovanov homology is a categorification of the Jones polynomial. In essence, it replaces the integer valued coefficients with vector spaces, diagrams with chain complexes and the polynomial with a bi-graded homology. We will discuss this construction here, working from the Kauffman state-sum formula. The result will be a bigraded chain complex whose Euler characteristic is the Jones polynomial of the related link. We now recall some algebraic preliminaries regarding graded modules.

### 3.1 Graded Modules

**Definition 3.1.1.** Let  $M = \bigoplus M_k$  for  $k \in \mathbb{Z}$  be a graded  $\mathbb{Z}$ -module where  $M_k$  represents the  $k$ -th graded component of  $M$ . The quantum dimension of  $M$  is the power series

$$q \dim(M) = \sum_{k \in \mathbb{Z}} \text{rank}(M_k) q^k$$

where  $\text{rank}(M_k) = \dim_{\mathbb{Q}}(M_k \otimes \mathbb{Q})$ .

The quantum dimension satisfies the following properties

$$q \dim(M \oplus N) = q \dim M + q \dim N$$

$$q \dim(M \otimes N) = q \dim M \cdot q \dim N$$

**Definition 3.1.2.** Let  $q^l$  for  $l \in \mathbb{Z}$  be the degree shift operator. That is, if  $M = \bigoplus M_k$ , then  $q^l M$  is the graded module given by  $(q^l M)_{k+l} = M_k$ . Then we have that  $q \dim(q^l M) = q^l(q \dim M)$ .



**Definition 3.1.3.** Let  $M = \bigoplus_j M_j$  and  $N = \bigoplus_j N_j$  be graded  $\mathbb{Z}$ -modules where  $M_j$  and  $N_j$  denote the  $j$ -th graded component of  $M$  and  $N$ , respectively. A  $\mathbb{Z}$ -module map  $f : M \rightarrow N$  is said to be graded with degree  $d$  if  $f(M_j) \subset N_{j+d}$ . A module map is called degree preserving (or grading preserving) if it is graded of degree zero. A graded chain complex is a chain complex for which the chain groups are graded  $\mathbb{Z}$ -modules and the differentials are graded.

**Definition 3.1.4.** Let  $[s]$ ,  $s \in \mathbb{Z}$ , be the height shift operation on chain complexes. That is, if  $C$  is a chain complex,  $\cdots \rightarrow C^i \rightarrow C^{i+1} \rightarrow \cdots$  of modules, then  $C[s]^r = C^{r-s}$  with all differentials shifted accordingly.

**Definition 3.1.5.** The graded Euler characteristic  $\chi_q(C)$  of a graded chain complex  $C$  is the alternating sum of the graded dimension of its homology groups

$$\chi_q(C) = \sum_i (-1)^i q \dim(H^i).$$

## 3.2 Khovanov's Construction

Let  $L$  be a link and  $D$  its planar projection. Let  $n$  be the number of crossings in the projection, with  $n_+$  ( $n_-$ ) the number of positive (negative) crossings. Our goal is to create a chain complex whose graded Euler characteristic agrees with the Jones polynomial. Recalling Kauffman's state-sum formula, there is a correspondence between elements of  $\{0, 1\}^n$  and states for the given diagram, allowing us to write the state-sum formula as follows

$$\langle D \rangle = \sum_{\text{states}} (-1)^{r(s)} q^{r(s)} (q + q^{-1})^{k(s)}.$$

We can rewrite the state-sum formula by collecting terms based on the number of 1 resolutions

$$\langle D \rangle = \sum_{i=0}^n (-1)^i q^i \sum_{\text{states} | r(s)=i} (q + q^{-1})^{k(s)}.$$

To each state, instead of associating the term  $(q + q^{-1})^{k(s)}$ , we will associate a graded module whose quantum dimension is  $(q + q^{-1})^{k(s)}$ . This is accomplished using the following procedure. Let  $A$  be the  $\mathbb{Z}$ -module generated by 1 and  $x$  with  $|1| = 1$  and  $|x| = -1$ . This gives  $q \dim(A) = q + q^{-1}$ . Using the tensor properties of quantum

dimension, it is easily seen that  $q \dim A^{\otimes k} = (q + q^{-1})^k$ . Thus, to each state  $s$ , we associate the module  $A^{\otimes k(s)}$ . Now to fit these pieces into a chain complex,  $C^{*,*}(D)$ . Following the rewritten state-sum formula, we will separate states into different homological degrees determined by number of 1 resolutions present in the state. So  $C^{i,*}(D) = q^i \bigoplus_{\text{states } |r(s)=i} A^{\otimes k(s)}$ . This chain complex has support in homological degrees  $0 \leq i \leq n$ . One refers to this chain complex as the ‘‘cube’’ of resolutions, thinking of each state as giving a ‘‘vertex’’ of the cube.

Now we must associate graded differentials, known as edges, to the cube. The differential on the chain complex will be constructed by assembling maps between specific states. For states  $s_1, s_2 \in \{0, 1\}^n$ , we say that  $s_1 \leq s_2$  if each entry of  $s_1$  is less than or equal to the corresponding entry of  $s_2$ . For example,  $010011 \leq 110011$ . We place a non-zero differential,  $d_{s_1, s_2}$ , between two states  $s_1, s_2$  if  $s_1 \leq s_2$  and  $r(s_2) = r(s_1) + 1$ , that is  $s_2$  has one more 1 than  $s_1$ . Two such diagrams differ only locally at the crossing where the states have differing resolutions. This difference is easily seen to be either an increase or decrease in the number of circles present by one. If the number of circles decreases, we say there is a merge between the states and if the number of circles increases, we say there is a split between the states. To a merge, we associate the (grading preserving) map  $m : A \otimes A \rightarrow qA$  given by

$$m(1, 1) = 1 \quad m(1, x) = m(x, 1) = x \quad m(x, x) = 0.$$

To a split, we associate the (grading preserving) map  $\Delta : A \rightarrow qA \otimes A$  given by

$$\Delta(1) = 1 \otimes x + x \otimes 1 \quad \Delta(x) = x \otimes x.$$

These two maps turn  $A$  into a commutative Frobenius algebra. Such an algebra satisfies the following commutative diagrams:

$$\begin{array}{ccc} A \otimes A \otimes A & \xrightarrow{m \otimes Id} & A \otimes A \\ Id \otimes m \downarrow & & \downarrow m \\ A \otimes A & \xrightarrow{m} & A \end{array} \qquad \begin{array}{ccc} A & \xrightarrow{\Delta} & A \otimes A \\ \Delta \downarrow & & \downarrow \Delta \otimes Id \\ A \otimes A & \xrightarrow{Id \otimes \Delta} & A \otimes A \otimes A \end{array}$$

$$\begin{array}{ccc} A \otimes A & \xrightarrow{\Delta \otimes Id} & A \otimes A \otimes A \\ Id \otimes \Delta \downarrow & \searrow m \circ \Delta & \downarrow Id \otimes m \\ A \otimes A \otimes A & \xrightarrow{m \otimes Id} & A \otimes A \end{array}$$

Thus we can assign differentials to the chain complex using the merge or split on the appropriate tensor factors and identity maps on the rest. As seen from the com-

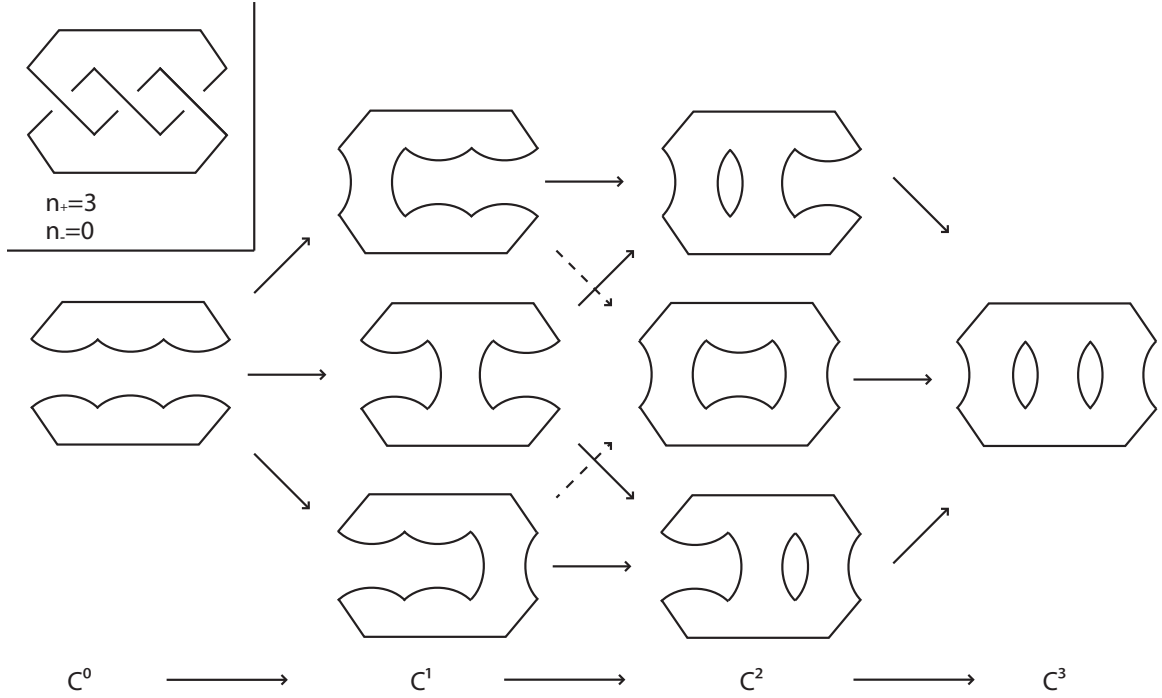


Figure 3.1: Chain Complex for the Trefoil Knot

mutation of the Frobenius algebra, signs are needed to create an actual differential. To do this, we need to consider each “face” of the cube. Two states  $s_1, s_2$  contribute a face to the cube if  $s_1 \leq s_2$  and  $r(s_2) = r(s_1) + 2$ . This means that the states differ in only two crossing locations where the two crossings are changed from a 0 resolution in  $s_1$  to a 1 resolution in  $s_2$ . There are two intermediate states, each with one 1 and one 0 resolution, in between  $s_1$  and  $s_2$ . By inspection, the two paths from  $s_1$  to  $s_2$  must constitute one part of the relations held by any Frobenius algebra. So each face in the (unsigned) cube of resolution commutes. In order to turn the maps into a proper differential, we can simply make each face anticommute. This can be done systematically. To do so, one chooses an order on the  $n$  crossings of the diagram. We can then give the current maps signs in the following way. Suppose  $s_1 \leq s_2$  and differ only in entry  $j$ . The differential will have the sign  $(-1)^{f(s_1, s_2)}$  where  $f(s_1, s_2)$  is the number of 1’s in the resolution that appear prior to entry  $j$  in the given ordering.

This construction is diagram dependent. Just as the Jones polynomial needs a writhe correction term, this construction needs an overall normalization to be a link

invariant. We denote this normalized chain complex as

$$\mathcal{C}(D) = q^{n_+ - 2n_-} C[n_-]$$

The homology groups of the shifted complex we denote by  $\mathcal{H}^i(D)$ . Thus

$$\mathcal{H}^{i,j}(D) = H^{i-n_-, j-n_++2n_-}(D).$$

**Theorem 3.2.1.** (*[Kho00], [BN05]*) *The homology groups  $\mathcal{H}^i(D)$  are independent of the choice of planar projection  $D$ . Furthermore, the graded Euler characteristic of the complex  $\mathcal{C}(D)$  is equal to the Jones polynomial of the link  $L$ .*

Hence we can write  $\mathcal{H}(L)$  and call  $\mathcal{H}^i(L)$  the homology groups of  $L$ . The homology groups for a knot do not depend on the orientation of the knot.

### 3.3 Properties of Khovanov Homology

This construction enjoys some nice properties relative to operations on diagrams of knots. We list them here.

**Proposition 3.3.1.** *For an oriented link  $L$ ,*

$$\mathcal{H}^{i,j}(L) = 0$$

*if  $i < n_-$ ,  $i > n_+$ , or  $j + 1 \equiv |L| \pmod{2}$ .*

This proposition says that the homology can only be nonzero for homological degrees between  $n_-$  and  $n_+$  and  $q$ -gradings which match the parity of the number of components of the link. We introduce the Poincaré polynomial for Khovanov homology, which we will denote  $Kh(L)(q, t)$ , as a compact way to display the homology of the link. The polynomial is defined as follows

$$Kh(L)(q, t) = \sum_{i,j} t^i q^j \dim(\mathcal{H}^{i,j}(L))$$

With this notation, the relation to the Jones polynomial is given by  $Kh(L)(q, -1) = J_L(q)$ .

The Khovanov homology of a link is often represented by a grid labeled homological and quantum gradings in the horizontal and vertical directions, respectively.

9				1
7				
5			1	
3	1			
1	1			
	0	1	2	3

Figure 3.2:  $Kh(\text{Trefoil}) = q^1 + q^3 + t^2q^5 + t^3q^9$

The darkened squares represent the diagonals  $j - 2i = \sigma(K) \pm 1$ , where  $\sigma(K)$  is the signature of the knot.

The homology of alternating links was observed experimentally to occupy only two diagonals, which gives rise to the following definition regarding the “thickness” of a link.

**Definition 3.3.2.** Let  $L$  be a link and  $\mathcal{H}(L)$  its homology. Let

$$S = \{j - 2i \mid \mathcal{H}^{i,j}(L) \neq 0\}.$$

We define the Kh-width (referred to as width) of link to be  $|S|$ , that is the number of diagonals on which the homology is non-zero.

We call a knot Kh-thin if its homology occupies only two diagonals and Kh-thick otherwise. We have the following theorem due to Lee

**Proposition 3.3.3.** (*[Lee02]*) *Non-split alternating links are Kh-thin.*

This explains the phenomenon that many of the small crossing number prime knots have thin homology, as many of those knots are alternating. Khovanov has shown that determining the thickness of prime knots is enough to determine the thickness of all knots.

**Proposition 3.3.4.** (*[Kho03]*)  *$K_1 \# K_2$  is Kh-thick if and only if one of  $K_1$  and  $K_2$  is Kh-thick.*

This proposition follows from the more general result relating the homology of a connected sum of links to the homology of its components.

**Proposition 3.3.5.** (*[Kho00]*) *Let  $K_1$  and  $K_2$  be knots. Then the connected sum  $K_1\#K_2$  satisfies the following long exact sequence*

$$\begin{aligned} \rightarrow \mathcal{H}^{i-1,j-1}(K_1 \cup K_2) \rightarrow \mathcal{H}^{i-1,j-2}(K_1\#K_2) \rightarrow \mathcal{H}^{i,j}(K_1\#K_2) \rightarrow \\ \rightarrow \mathcal{H}^{i,j-1}(K_1 \cup K_2) \rightarrow \mathcal{H}^{i,j-2}(K_1\#K_2) \rightarrow \mathcal{H}^{i+1,j}(K_1\#K_2) \rightarrow \end{aligned}$$

The knot with smallest crossing number which does not have thin homology is the knot  $9_{42}$ . The figure 3.3 shows the Khovanov homology of the knot. The darkened lines are again the signature diagonals and the dark square is meant to highlight the nonzero homology off the signature diagonal.

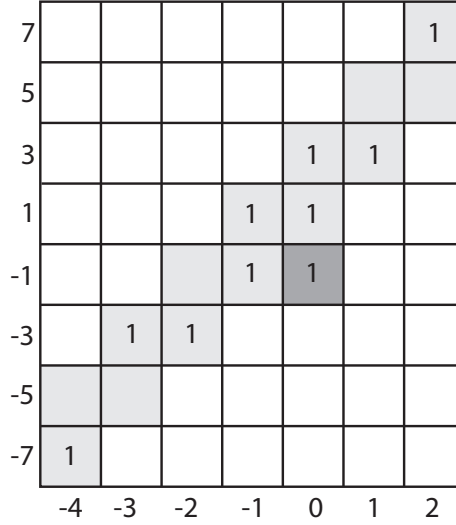


Figure 3.3:  $Kh(9_{42}) =$

$$t^{-4}q^{-7} + t^{-3}q^{-3} + t^{-2}q^{-2} + t^{-1}q^{-1} + t^{-1}q^1 + q^{-1} + q^1 + q^3 + t^1q^3 + t^2q^7$$

Given a knot  $K$  with a distinguished positive crossing, there is a long exact sequence involving the diagrams obtained from the 0 resolution  $K_0$  and 1 resolution  $K_1$  of the distinguished crossing. The unnormalized long exact sequence is given by

$$\begin{aligned} \rightarrow H^{i-1,j-1}(K_1) \rightarrow H^{i,j}(K) \rightarrow H^{i,j}(K_0) \rightarrow \\ \rightarrow H^{i,j-1}(K_1) \rightarrow H^{i+1,j}(K) \rightarrow H^{i+1,j}(K_0) \rightarrow . \end{aligned}$$

For a positive crossing, the 0 resolution is oriented and the 1 resolution is unoriented. Thus we can choose the corresponding orientation for  $K_0$  and an arbitrary orientation for  $k_1$ . If we let  $c = n_-(K_0) - n_-(K)$  the long exact sequence has the following for on the normalized homology

$$\begin{aligned} &\rightarrow \mathcal{H}^{i-c-1, j-3c-1}(K_1) \rightarrow \mathcal{H}^{i, j}(K) \rightarrow \mathcal{H}^{i, j-1}(K_0) \rightarrow \\ &\rightarrow \mathcal{H}^{i-c, j-3c-1}(K_1) \rightarrow \mathcal{H}^{i+1, j}(K) \rightarrow \mathcal{H}^{i+1, j-1}(K_0) \rightarrow . \end{aligned}$$

Similarly for a distinguished negative crossing with  $K_0$  the oriented resolution and  $K_1$  the unoriented resolution with  $c$  as above, we have the following long exact sequences

$$\begin{aligned} &\rightarrow \mathcal{H}^{i, j-1}(K_0) \rightarrow \mathcal{H}^{i, j}(K) \rightarrow \mathcal{H}^{i-c-1, j-3c-1}(K_1) \rightarrow \\ &\rightarrow \mathcal{H}^{i+1, j-1}(K_0) \rightarrow \mathcal{H}^{i+1, j}(K) \rightarrow \mathcal{H}^{i-c, j-3c-1}(K_1) \rightarrow . \end{aligned}$$

### 3.4 Lee Homology

In this section we will describe what is known as Lee homology. Lee proved that there is a modification to the differentials provided by Khovanov which results in another link homology. This homology does not capture the Jones polynomial and is instead much smaller. The homology is said to be “boring, but in an interesting way.” The modification is as follows. Lee defines additional differentials denoted with a prime. The maps  $\Delta' : A \rightarrow A \otimes A$  and  $m' : A \otimes A \rightarrow A$  are 0 except for

$$\Delta'(x) = 1 \otimes 1 \quad m'(x \otimes x) = 1$$

Lee shows that these maps commute with the given  $\Delta$  and  $m$ . This means that, with the sign assignment,  $\Delta + \Delta'$  and  $m + m'$  can be used to form a new differential,  $d'$  on the same cube of resolutions. The new differential  $d'$  is not grading preserving. The Khovanov differentials preserve grading, but the Lee differential increase grading by 4. So instead of a bigraded homology theory, we get a filtered homology theory denoted  $\mathcal{H}_{Lee}$ . With this setup, Lee proves the following

**Proposition 3.4.1.** *For a link  $L$ ,  $\mathcal{H}_{Lee}(L)$  has rank  $2^{|L|}$ .*

Each pair of homology classes corresponds precisely to an orientation  $o$  of the chosen link  $L$ . For each orientation  $o$  of a link diagram  $D$ , there is a corresponding oriented resolution  $O(D)$  which contributes a summand in the Khovanov chain complex. She shows that the oriented resolutions of a link provide special state-cycle representatives for the Lee homology. These are representatives of minimal quantum filtration grading. To find the actual filtration grading of the cycles, one must determine the highest filtration grading which contains cycle representatives. To do this, one must consider a minimax type computation, which is typically difficult to do by inspection. We will describe these elements in detail in chapter 4.

**Proposition 3.4.2.** *The homological gradings of the Lee homology elements are determined by the linking number  $\ell(L_1, L_2)$  for each pair of link components  $L_1$  and  $L_2$ .*

This means that for a knot, the homology consists of two pieces in homological degree 0. Rasmussen proved that these two pieces in fact differ by 2 degrees in the associated graded of the induced quantum filtration grading on homology. The average of the filtration of these pieces is then an invariant which can be read from Lee homology. We call this integer the  $s$ -invariant, denoted  $s(K)$ .

**Proposition 3.4.3.** (*[Ras04]*) *For a knot  $K$ ,*

$$|s(K)| \leq 2g_4(K)$$

*where  $g_4(K)$  is the smooth 4-ball genus of the knot.*

This construction by Lee can also be interpreted as giving a spectral sequence whose first page is  $E_1^{i,j} = \mathcal{H}_{Kh}^{i,j}(L) \otimes \mathbb{Q}$  which converges to  $E_\infty^{i,j} = \mathcal{H}_{Lee}(L)$ . For a knot,  $K$ , the spectral sequences converges to  $E_\infty = \mathbb{Q} \oplus \mathbb{Q}$ . Specifically,  $E_\infty^{0,s\pm 1} = \mathbb{Q} \oplus \mathbb{Q}$  where the even integer  $s$  is Rasmussen's invariant. The differentials in the spectral sequence on page  $i$  are of bidegree  $\{1, 4i\}$ . It is conjectured that this spectral sequence always converges after the second page. This spectral sequence is useful for many computational purposes, especially when combined with the above long exact sequences. We show in figure 3.4 the differential pairings of the spectral sequence for the Lee homology of the  $9_{42}$  knot. The remaining terms after cancellation appear in filtration gradings  $\pm 1$ , meaning  $s(9_{42}) = 0$ .



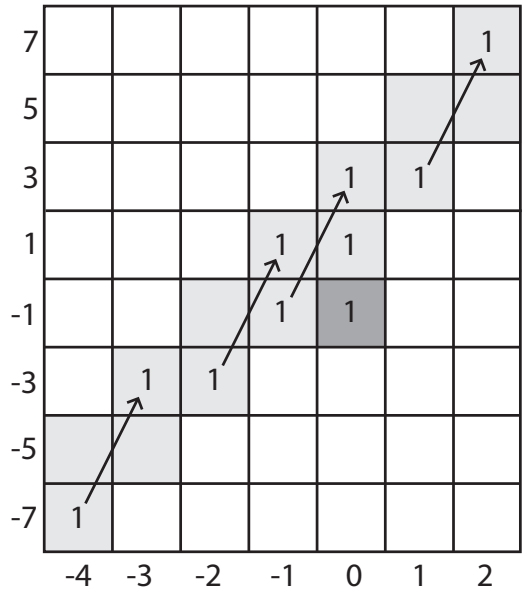
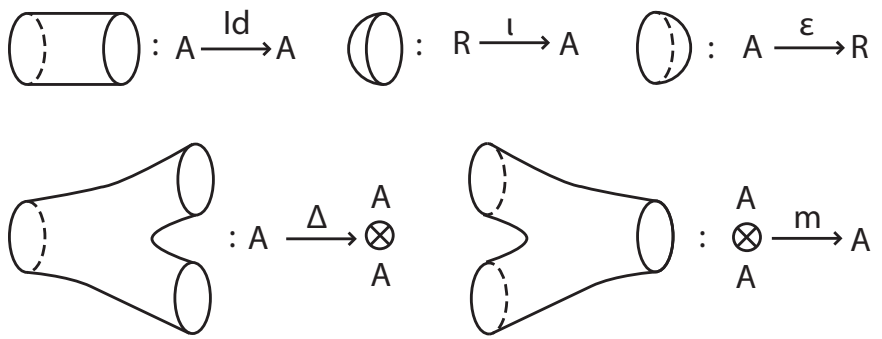


Figure 3.4: The spectral sequence cancellation of  $\mathcal{H}(9_{42})$

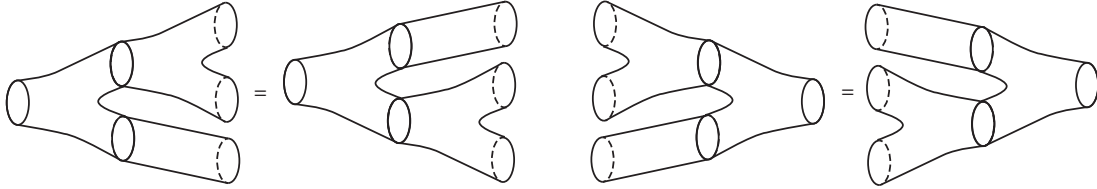
### 3.5 A Categorical Formulation

#### Encapsulating Khovanov and Lee Homology

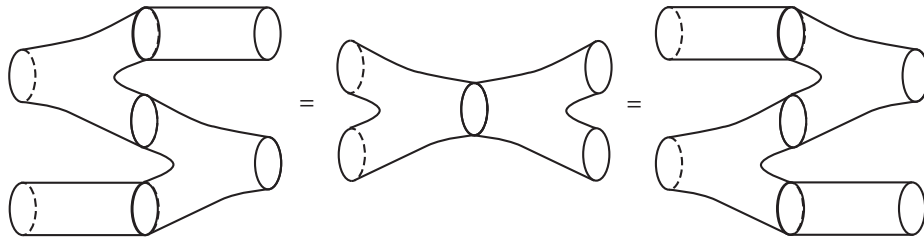
Both Khovanov and Lee homology have nice geometric interpretations as described by Bar-Natan in [BN05]. Khovanov’s original description was based of a certain Frobenius algebra. Frobenius algebras over a commutative ring  $R$  are well known to be the same thing as representations of the monoidal category  $Cob_{1+1}$  of cobordisms into the tensor category  $Mod - R$ . This shows that the category  $Cob_{1+1}$  is equivalent to the free tensor category on a single Frobenius algebra object, namely the circle. As described before, a Frobenius algebra is an algebra  $A$  with maps  $Id, \Delta, m, \iota, \epsilon$  satisfying certain relations. The maps can be visualized as surfaces (maps between circles) in the following way



The surfaces are subject to relations up to isotopy the corresponding maps are subject to the relations those isotopies would impose. The commutative triangles explained previously can now be represented graphically. The algebra is both commutative and cocommutative



The algebra also satisfies the namesake Frobenius relation

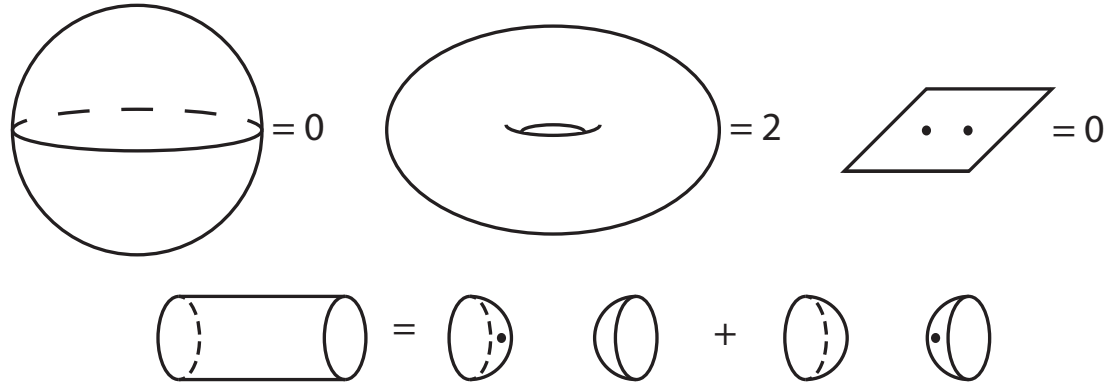


We can introduce an additive structure on  $Cob_{1+1}$  by taking linear combinations of morphisms to make the hom sets into abelian groups. Additionally, we can introduce formal direct sums of objects and write the Khovanov complex as a complex of objects from this category. The objects are actually represented by the Kauffman states themselves and the differentials correspond to split and merge surfaces. We don't have a homology theory, as there is no sense of kernel or image in this category, but the chain homotopy type of the complex is well defined. The Khovanov and Lee algebras can be viewed as surfaces, each having their own set of relations. Relations must be imposed to make the result homotopy invariant under Reidemeister moves. Dror Bar-Natan [BN07] determined the relations needed.

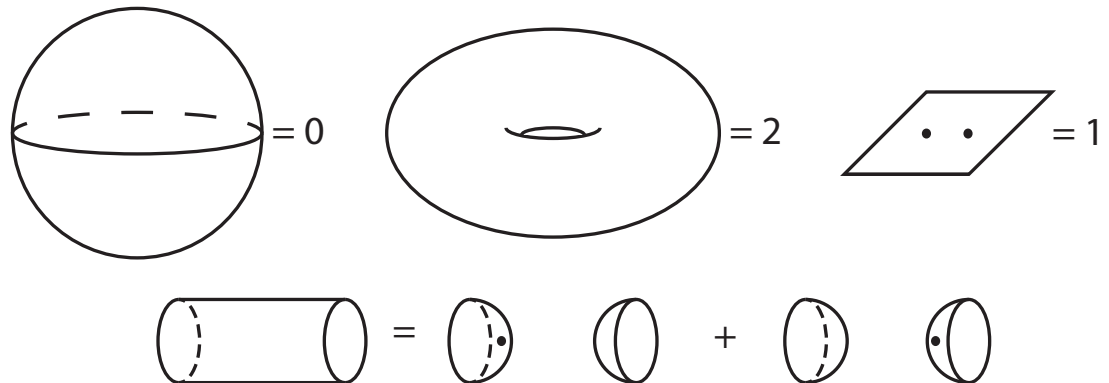
Before we describe the relations, we must introduce some shorthand notation for these surfaces. We let a dot on a surface represent one half of the related surface with genus.

$$\left( \begin{array}{c} \text{circle} \\ \text{with a dot} \end{array} \right) = \frac{1}{2} \left( \begin{array}{c} \text{circle} \\ \text{with a handle} \end{array} \right)$$

The relations needed for Khovanov homology are



while for Lee homology we need



The relations are very similar for Khovanov and Lee, the one difference being the double dot relation. We denote the sphere relation by  $S$ , and we call the relation at the bottom “neck-cutting”. These relations can be described through a universal version of the category. Instead of imposing an integer valued relation for a double dotted surface, we allow an indeterminate  $\alpha$  which corresponds to  $\frac{1}{8}$  of a closed genus-3 surface. We then have a base ring  $\mathbb{Z}[\alpha]$  for our the universal category. With the dotted surface relation above,  $\alpha$  is equivalent to a sphere with 3 dots. Using the neck cutting relation, we can pull pairs of dots off of surfaces and replace them with a coefficient  $\alpha$ .

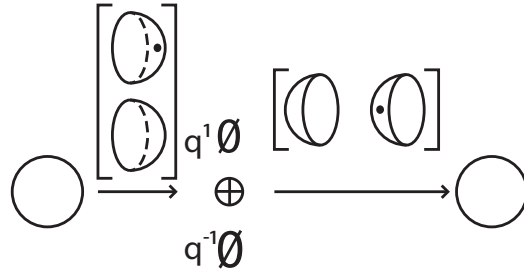
$$\text{Parallelogram with 2 dots} = \text{Sphere with dot and neck-cutting line} + \text{Sphere with dot and neck-cutting line} = \alpha \text{Parallelogram with 1 dot}$$

Using this relation, one can recover Khovanov homology by setting  $\alpha = 0$  and by Lee homology by setting  $\alpha = 1$ . The relation  $\alpha = 1$  is inhomogeneous.

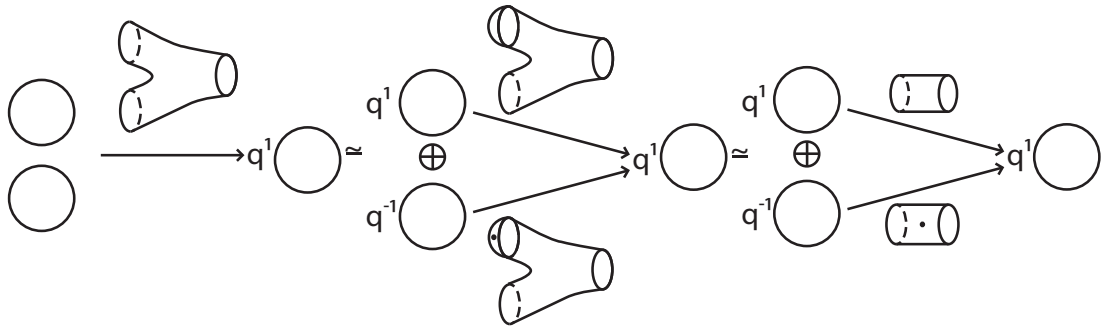
The categorical formulation of Khovanov homology allows for some computational advantages. Note that the category contains an empty 1–manifold as an object. With

the dotted surface structure, there is an isomorphism between a circle in the plain and two quantum grading shifted empty diagrams. This relationship is known as “delooping” and is due to Bar-Natan in [BN07].

**Lemma 3.5.1.** (*Bar-Natan*) *If a state  $S$  contains a closed loop  $l$ , then it is isomorphic to the direct sum of two copies  $q^1 S'$  and  $q^{-1} S'$  of  $S$  in which  $l$  is removed, one taken with a degree shift of  $+1$  and one with a degree shift of  $-1$ . The isomorphisms are as follows:*



This delooping isomorphism allows the chain complex to be simplified by removing circles from states. This isomorphism is also grading preserving, and thus no information is lost in delooping. The following figure shows how delooping can be used to simplify a chain complex.



The original map here was a merge between two circles. By delooping the the top circle, we get a homotopic chain complex with the top map being the identity morphism. This leads us to our next proposition. Using generalized linear algebra, we can remove inessential summands from the chain complex, potentially changing the remaining maps in the complex. We now introduce the Gaussian elimination lemma from [BN05].

**Lemma 3.5.2.** (*Bar-Natan*) *If  $\varphi : b_1 \rightarrow b_2$  is an isomorphism (in some additive category  $\mathcal{C}$ ), then the four term complex segment in  $Mat(\mathcal{C})$*

$$[C] \xrightarrow{\begin{pmatrix} \alpha \\ \beta \end{pmatrix}} \begin{bmatrix} b_1 \\ D \end{bmatrix} \xrightarrow{\begin{pmatrix} \varphi & \delta \\ \gamma & \epsilon \end{pmatrix}} \begin{bmatrix} b_2 \\ E \end{bmatrix} \xrightarrow{\begin{pmatrix} \mu & \nu \end{pmatrix}} [F]$$

is isomorphic to the direct sum of complexes

$$[C] \xrightarrow{\begin{pmatrix} 0 \\ \beta \end{pmatrix}} \begin{bmatrix} b_1 \\ D \end{bmatrix} \xrightarrow{\begin{pmatrix} \varphi & 0 \\ 0 & \epsilon - \gamma\varphi^{-1}\delta \end{pmatrix}} \begin{bmatrix} b_2 \\ E \end{bmatrix} \xrightarrow{\begin{pmatrix} 0 & \nu \end{pmatrix}} [F]$$

This lemma allows us, in combination with delooping, to remove inessential pieces of chain complexes before computing homology at the cost of modifying some differentials. Each of the differentials in the Khovanov complex is graded, the “new” differential given by  $\epsilon - \gamma\varphi^{-1}\delta$  will be of homogeneous degree. Using this elimination lemma we can simplify the example complex even further to obtain the following:

Simplifications like the one above lead to Khovanov homology being readily computable. In fact, the KnotTheory‘ package provided by Bar-Natan and Morrison is able to compute Khovanov homology for knots of under 40 crossings in seconds and knot under 100 crossings in a reasonable amount of time. The results on these computations for knots with small crossing number are displayed at [katlas.org](http://katlas.org) [MBN] thanks to Bar-Natan and Morrison.

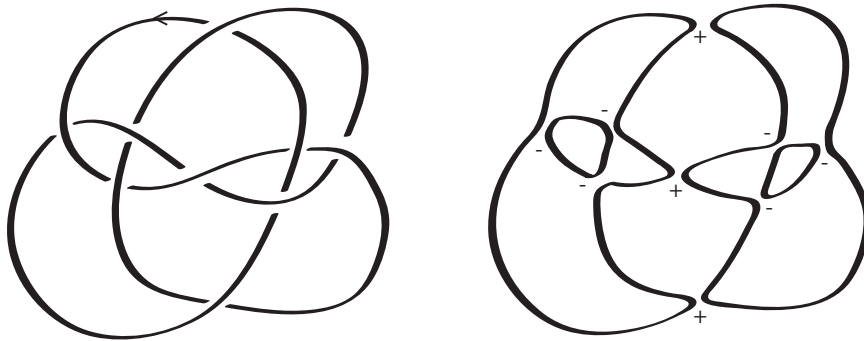
# Chapter 4

## Bounds on Rasmussen's Invariant

In this chapter we will create chain maps to obtain bounds on Rasmussen's  $s$ -invariant. By using maps instead of other techniques, we also obtain actual states which realize these bounds. In general, the  $s$ -invariant of a knot is hard to compute. It is conjectured that the  $s$ -invariant can be read from the Poincaré polynomial corresponding to the homology of the knot. We can compute the the  $s$ -invariant in certain cases: positive knots and alternating knots. For a positive knot  $K$ ,  $\mathcal{H}^{0,j}(K) = \mathbb{Q}$  for  $j = s(K) \pm 1$  and is 0 otherwise. So for a positive knot, the  $s$ -invariant can be read from the  $t = 0$  term of the Poincaré polynomial. For alternating knots, the support of the Khovanov homology was shown to be precisely the signature diagonals. In this case,  $s(K) = \sigma(K)$ . We generalize the technique for calculating the  $s$ -invariant for positive diagrams to general diagrams. The technique will provide bounds, upper and lower, on the  $s$ -invariant of a knot, dependent on the diagram. Andrew Lobb provides bounds on the  $s$ -invariant which agree with our bounds. His techniques are non-constructive, however. Tetsuyo Abe has determined when these bounds are sharp. Our technique will not only calculate the  $s$  invariant in these situations, but will provide generators for the Lee homology as well.

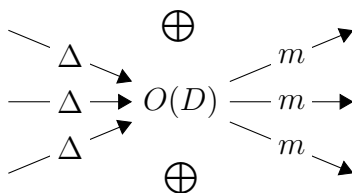
### 4.1 Lee Homology and Oriented Resolutions

Our goal is to create a chain map  $C(U) \rightarrow C(D)$ , from an oriented diagram of the unknot to an oriented diagram of another knot. Investigating the degree of this map will allow us to give bounds on Rasmussen's  $s$  invariant of the associated knot. We

Figure 4.1: The oriented resolution of the knot  $9_{40}$ 

will do so by composing maps piece by piece to obtain the final desired map. First, we describe Lee homology in more detail. Given an oriented diagram  $D$  of a link  $L$ , we write  $O(D)$  to represent the oriented resolution of the diagram. In the Khovanov construction, this corresponds to taking the 0 resolution at all positive crossings and 1 resolution at all negative crossings in the diagram. One should also note that the oriented resolution contributes a summand in the Khovanov chain complex in homological degree 0.

The direct summand of  $C(D)$  corresponding to the oriented resolution has a few special properties. It has  $n_-$  incoming maps and  $n_+$  outgoing maps. Each of the incoming maps is a split map  $\Delta$  over a negative crossing and each of the outgoing maps is a merge map  $m$  over a positive crossing.



Lee used these observations to provide generators for Lee homology. The original basis for Khovanov's algebra was given by the graded elements 1 and  $x$ . Lee changes basis to  $a = 1 + x$  and  $b = 1 - x$ , which are orthogonal ( $m(a, b) = 0$ ) in Lee homology. Given a knot diagram  $D$  with orientation  $o$ , the oriented resolution state  $O(D)$  contributes a direct summand to the Khovanov complex. We can label this state with the alternating tensor products  $s_o = a \otimes b \otimes a \otimes \cdots \otimes a$  and  $s_{\bar{o}} = b \otimes a \otimes b \otimes \cdots \otimes b$ , where adjacent circles all have opposite labels. Since each differential out of this

summand is a merge between adjacent circles, each of these states clearly represents a cycle. Lee shows that these cycles in fact generate homology. These are not necessarily the cycles which lie in the highest filtration grading possible. To determine the  $s$ -invariant, one must find homological representatives of highest filtration gradings.

Let us now consider a diagram with all positive crossings. The  $s$  invariant is known to have value  $n_+ - k + 1$ , where  $k$  is the number of circles in the oriented resolution. The two Lee canonical elements  $s_o$  and  $s_{\bar{o}}$  are the highest degree homological generators. Their sum and difference  $s_o \pm s_{\bar{o}}$  generate Lee homology and have quantum grading  $n_+ - k + 1 \pm 1$ . This is the basic idea behind the maps we wish to create. To construct our chain maps, we wish to copy this type of alternating state labeling to each “negative patch” in our diagram. So, we wish to construct maps which create this alternating label of circles in the oriented resolution. We want a set of maps  $\varphi : \circ \rightarrow \circ\circ$  which achieve this alternating labeling. The second tensor factor indicates the newly labeled circle.

$$\begin{aligned}\varphi_A(a) &= a \otimes b, \varphi_A(b) = -b \otimes a \\ \varphi_O(a) &= a \otimes 1, \varphi_O(b) = b \otimes 1 \\ \varphi_D(a) &= a \otimes b, \varphi_D(b) = b \otimes a\end{aligned}$$

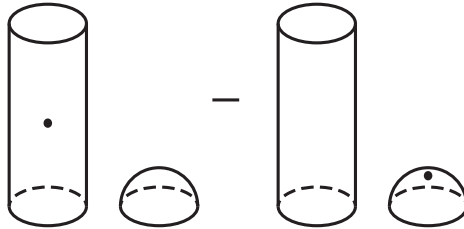
The maps  $\varphi_A$  and  $\varphi_D$  appear similar, but their realizations will become apparent shortly. We will also need adjoint maps  $\varphi' : \circ\circ \rightarrow \circ$  which behave well with alternating labels as inputs to construct our inverse chain maps. We would ideally like maps which behave in the following way:

$$\begin{aligned}\varphi'_A(a \otimes a) &= 0, \varphi'_A(a \otimes b) = -2a, \varphi'_A(b \otimes a) = -2b, \varphi'_A(b \otimes b) = 0 \\ \varphi'_O(a \otimes a) &= a, \varphi'_O(a \otimes b) = -a, \varphi'_O(b \otimes a) = b, \varphi'_O(b \otimes b) = -b \\ \varphi'_D(a \otimes a) &= 0, \varphi'_D(a \otimes b) = -2a, \varphi'_D(b \otimes a) = 2b, \varphi'_D(b \otimes b) = 0\end{aligned}$$

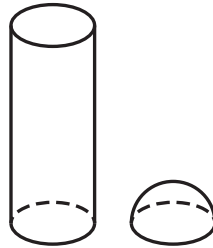
These maps can be achieved using cobordisms in Lee’s category. Working in Lee’s category means that we can remove double dots from a surface. We will adopt the notation that a map with an overline is a dotted version of that map. We will use this notation only when there is only one connected component. For example  $\overline{Id}$  is the identity map with a dot. With the Lee local relations in place,  $\overline{\overline{f}} = f$  for any



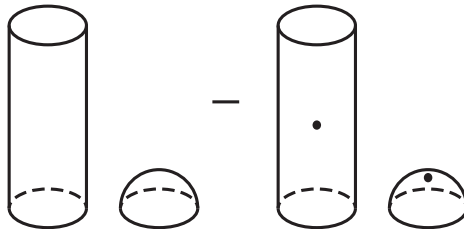
map  $f$ , since the two dots can be isotoped across the connected component and then cancel. We now introduce maps that we will use in our construction. Let us consider the map  $\varphi_A : \circ \rightarrow \circ\circ$



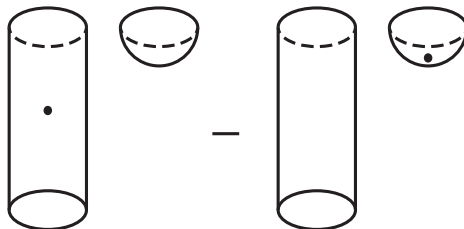
The map  $\varphi_A$  will take a state and label the newly born circle with the alternate state. The name is meant to indicate this assignment. This map has filtration degree  $-1$ . We also consider the map  $\varphi_O : \circ \rightarrow \circ\circ$  given by



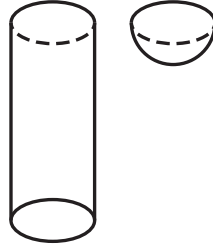
This map will assign the value 1 to a newly born circle, hence the name  $\varphi_O$ . This map has filtration degree 1. We will also need a third map,  $\varphi_D : \circ \rightarrow \circ\circ$  given by



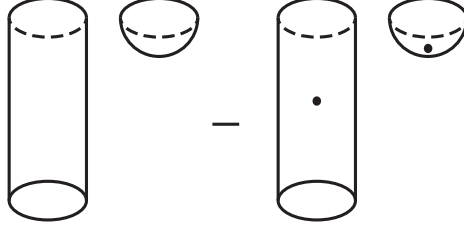
Note that the map  $\varphi_D$  is the map  $\varphi_A$  postcomposed with a dotted identity map on one of the components. This map is not homogeneous and has filtration degree  $-3$ . We will also need the adjoint versions of these maps to create an inverse map. Let us consider the map  $\varphi'_A : \circ\circ \rightarrow \circ$



We also consider the map  $\varphi'_O : \circ\circ \rightarrow \circ$  given by



the inversion of the third map,  $\varphi'_D : \circ\circ \rightarrow \circ$  is given by



Note the subtle sign differences among the maps. The maps  $\varphi_A$  and  $\varphi_D$  are closely related, as are  $\varphi'_A$  and  $\varphi'_D$ . We now investigate the interaction between these maps and their compositions. We illustrate one of the compositions graphically. Consider the composition  $\varphi'_A \circ \varphi_A$ . The figure 4.2 shows the composition and cancellation of pieces using the Lee relations.

This shows that the composition of  $\varphi_A$  with  $\varphi'_A$  gives the map  $-2\overline{Id}$ . Using similar cancellations and isotopies results in the following list of compositions:

$$\varphi'_A \circ \varphi_A = -2\overline{Id}$$

$$\varphi'_A \circ \varphi_O = -Id$$

$$\varphi'_A \circ \varphi_D = -2Id$$

$$\varphi'_O \circ \varphi_A = -\overline{Id}$$

$$\varphi'_O \circ \varphi_O = 0$$

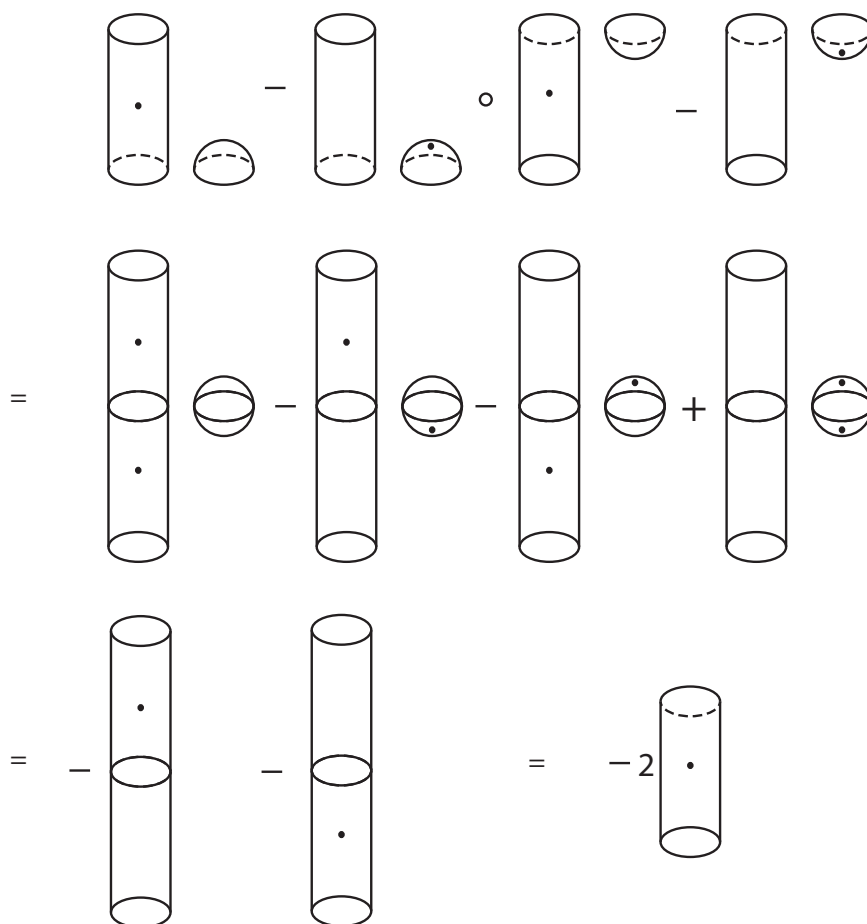
$$\varphi'_O \circ \varphi_D = -Id$$

$$\varphi'_D \circ \varphi_A = -2Id$$

$$\varphi'_D \circ \varphi_O = -\overline{Id}$$

$$\varphi'_D \circ \varphi_D = -2\overline{Id}$$

This list of compositions will enable us to simplify the proofs later. One should keep in mind that we are working over  $\mathbb{Q}$  so the powers of 2 and the signs appearing

Figure 4.2: The composition  $\varphi'_A \circ \varphi_A$

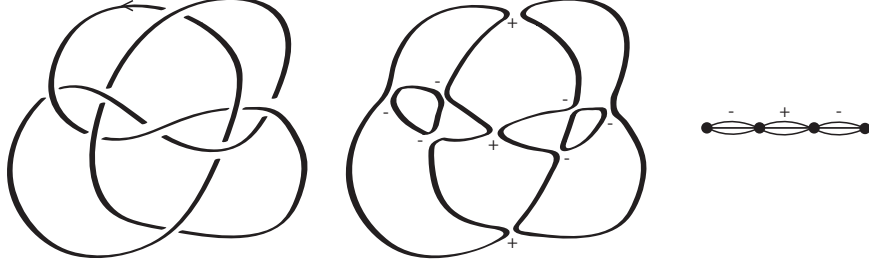


Figure 4.3: The Seifert graph of the knot  $9_{40}$

in the compositions will ultimately be invertible. We now make a few notes about the behavior of these maps with the differential maps appearing in the Khovanov complex, namely  $\Delta$  and  $m$ . The maps  $\varphi_A$  and  $\varphi_D$  are specifically constructed so that the composition  $m \circ \varphi_A = 0$  and  $m \circ \varphi_D = 0$ . Their respective adjoint maps are also constructed so that  $\varphi'_A \circ \Delta = 0$  and  $\varphi'_D \circ \Delta = 0$ . That is, these maps were created to behave well with the special properties of the direct summand corresponding to the oriented resolution.

## 4.2 Construction of the chain maps

We will construct the chain maps using the  $\varphi$  maps described in the earlier sections. To avoid adding extra grading shifts to the calculation, we will work with an unshifted version of the Khovanov complex. We will leave out the final  $q$ -grading shift of  $q^{w(D)}$ . This formal shift simply changes the quantum gradings of each piece of the chain complex as well as the corresponding filtration gradings in the Lee complex. The direct summand corresponding to the oriented resolution will be the source and target of our chain map. We will now define graphs associated to an oriented resolution which will allow us to construct our maps algorithmically.

**Definition 4.2.1.** To an oriented resolution  $O(D)$  corresponding to a diagram  $D$ , we can assign a decorated graph  $T(D)$ , called the **Seifert graph**, in the following manner:

For each circle in  $O(D)$  we add a vertex to the graph. Each crossing in  $D$  is incident to two circles in  $O(D)$ . For each positive crossing in  $D$ , we add the corresponding edge to  $T(D)$  assigned with  $+$ . For each negative crossing in  $D$ , we add the corresponding

edge to  $T(D)$  assigned with  $-$ .

A few notes about Seifert graphs. A crossing in diagram will always correspond to an edge between distinct vertices. This means that the graph will have no edges which start and end at the same vertex. The Seifert graph will also contain no cycles of odd length. This is due to the fact that the circles in the oriented resolution can naturally be given an orientation that agrees with the original orientation of the diagram. An odd length cycle would force a loop to have two different orientations. These two facts combined tell us that Seifert graphs are bipartite. The vertices can be separated into two groups, those whose corresponding loops inherit a clockwise orientation and those that inherit a counterclockwise orientation. Observed locally, it is clear that a crossing must be incident to two circles of opposite orientation.

**Definition 4.2.2.** To a Seifert graph  $T(D)$  we can associate two graphs:

The graph  $T^+(D)$  is formed by removing all negative ( $-$ ) edges from  $T(D)$  and  $T^-(D)$  is formed by removing all positive ( $+$ ) edges from  $T(D)$ .

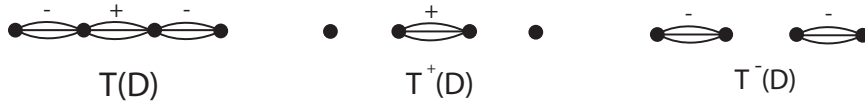


Figure 4.4: Associated Seifert graphs of the knot  $9_{40}$

We now introduce some terminology for Seifert graphs and their associated subgraphs. We will say that two vertices in  $T(D)$  are positively (negatively) connected if at least one of the edges between them in  $T(D)$  are marked with a plus (minus). We say that two vertices in  $T(D)$  are strictly positively (negatively) connected if all connections between them are positive (negative).

For the graph  $T^+(D)$ , we choose a spanning forest (a collection of trees), called  $F^+(D)$ . Similarly, we choose a spanning forest  $F^-(D)$  for the graph  $T^-(D)$ . We will now use these graphs to define the desired chain map. Assign an ordering of the vertices in  $T^+(D)$ . We will do this as follows. Pick a vertex in  $T^+(D)$  (preferably one with an edge connecting to it). Label that vertex with a 1. Label all adjacent vertices 2, 3,  $\dots$  consecutively in some arbitrary way. Move to the next lowest numbered vertex and label all unlabeled adjacent vertices. Proceed until all connected

vertices are labeled, then move to a new connected component and repeat with the next available label.

These spanning forests will give us directions for creating our chain map. We define the chain map in the following fashion. We will describe this as an algorithm, exhausting the vertices in order. At each step, we will add a map to the total composition. The algorithm for constructing the chain map based on the choice of spanning forests.

We start with vertex 1 of  $T^+(D)$ . The circle in  $O(D)$  corresponding to this vertex will be the starting point of our map. The initial step of the composition will be to map the chosen (crossingless) unknot to this circle using an identity cobordism. We now describe the algorithm for exhausting the forest. We consider a vertex exhausted once we have prescribed a morphism to the corresponding circle in  $O(D)$ . What we describe will be a way of mapping elements from the unknot complex to the complex corresponding to  $D$ . We will show later that this is indeed a chain map.

Algorithm: For each edge in  $F^+(D)$  connected to the current vertex, we add a composition to our map using the state copying map,  $\varphi_A$ , above. To do this, we create the map for this stage of the composition by taking the identity map on all previously added components and by using the map  $\varphi_A$  to add the circle corresponding to the latest vertex to the map. The vertices are positively connected because they are connected by an edge in  $T^+(D)$ .

Once we have exhausted the edges in the current tree, we choose another tree in the forest. We add the first circle of the new connected component using the  $\varphi_O$  map. This composition can be done from any previously added vertex. We then add each connected vertex using the  $\varphi_A$  map as above.

We continue this process until the only remaining forests are single vertices. Once each edge from the spanning forest has been accounted for, we must consider each of the vertices left in the  $T^-(D)$ . They have no positive edges connected to them in the graph, so they are not involved in any outgoing merge maps. Thus, for each remaining vertex, we use the map  $\varphi_O$  to add that vertex to the current composition. This will account for all of the circles in the diagram. All that remains is to show that this map is indeed a chain map. Call the resulting composition  $I : C(U) \rightarrow C(D)$ . Figure 4.5 shows the result of the construction for the given diagram of the  $4_1$  knot.

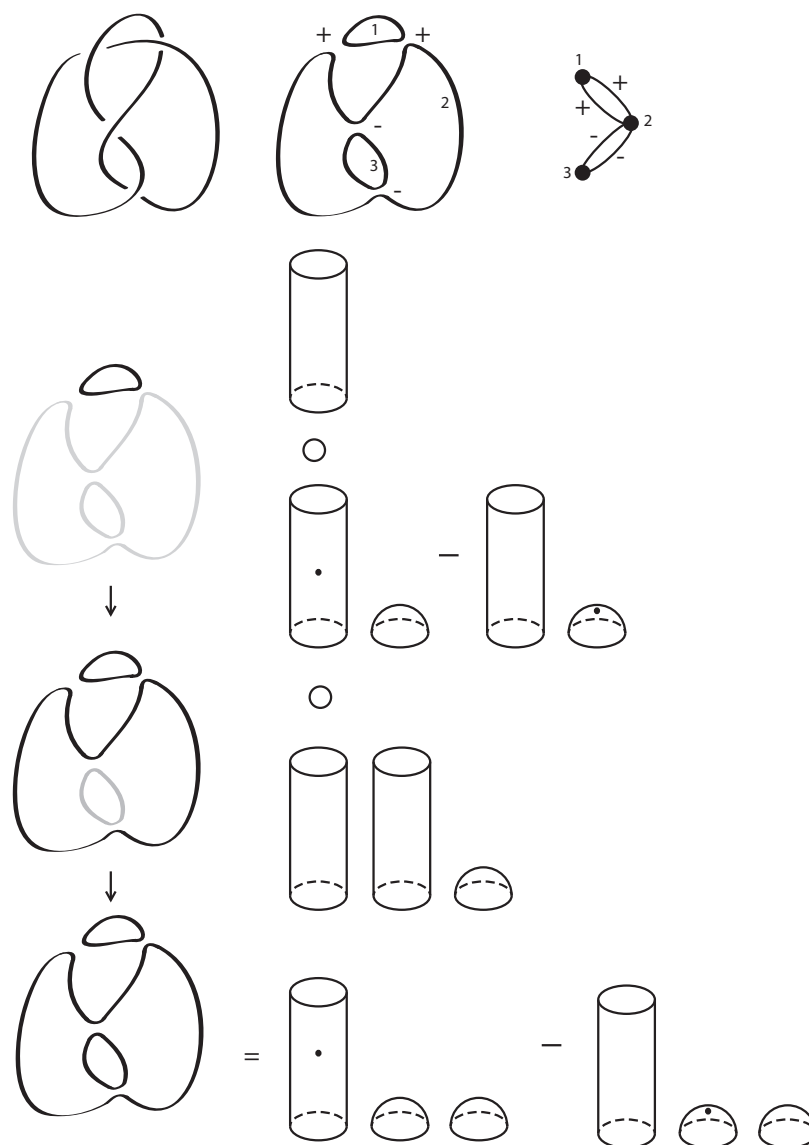


Figure 4.5: The resulting chain map  $I$  for the knot  $4_1$

We now discuss some properties of the resulting map. The composition, once simplified and once terms are collected, will be a map which is the identity on one component along with dotted and undotted caps to the remaining components. Typically, this map will have several terms. We begin with an observation about each positive component of the graph.

**Lemma 4.2.3.** *Suppose, in the construction of  $I$ , that two vertices share a positive edge. Let  $d_\alpha$  be the term of the differential in  $C(D)$  which corresponds to the merging of those two circles from the oriented resolution. Then  $d_\alpha \circ I = 0$ .*

*Proof.* We prove this using the basis  $a, b$  for the Lee homology of the unknot and by considering the first connected component. If we consider  $I(a)$ , we see that the state alternating map  $\varphi_A$  will alternate states to all adjacent circles. This means that the resulting image will be one term with alternating  $a$  and  $b$  labels on each of the circles. By construction, circles adjacent to each other which share a positive crossing will have opposite labellings, one with basis element  $a$  and one with basis element  $b$ . This is guaranteed by the fact that the graph has no odd cycles. By examining the Lee basis, we see that  $m(a, b) = 0 = m(b, a)$ . So  $d_\alpha \circ I = 0$ , since the circles must be labeled oppositely and this part of the differential is a merge of circles. Since the image of  $a$  or  $b$  under this composition  $d_\alpha \circ I$  are both 0, their sum and difference must also be 0. Since  $a + b = 2$ , the image of 1 under this map must also have this property. For all components beyond the first, we used the map  $\varphi_O$  in our construction, and hence the image on the first circle in the new component must be 1. Thus, for any two vertices that share a positive crossing, the term contributed to the composition with the differential is 0.  $\square$

This observation allows us to prove that  $I$  is indeed a chain map.

**Proposition 4.2.4.** *The constructed  $I$  is a map of filtered chain complexes, and hence of their associated graded complexes.*

*Proof.* We consider the Lee basis  $a, b$  again. By the above lemma, the resulting states  $I(a)$  and  $I(b)$  are both cycles of  $\mathcal{H}(D)$ . The composition  $I \circ d$  is trivial as all differentials in the chain complex of the unknot without crossings are 0. Thus  $d \circ I = 0 = I \circ d$ . So the map commutes with the differential and we have that  $I$  is indeed a chain map.  $\square$



The constructed map will only provide bounds for Rasmussen's invariant if this cycle actually represents a nonzero class in homology. We now show that this map is invertible, and hence the image is nontrivial. The map we construct from  $C(D)$  to  $C(U)$  will be a chain map. As before, we restrict ourselves to the direct summand of  $C(D)$  corresponding to the oriented resolution of  $D$ . To form a chain map out of  $C(D)$  the primary concern will be commutation with the incoming maps to the oriented resolution, which are all merge maps ( $m's$ ) associated to negative crossings. We will construct the map with choice made in our construction of  $I$ .

We now construct the map  $I' : C(D) \rightarrow C(U)$ . We still have our chosen spanning tree from the construction of  $I$ . We create our map from compositions vertex by vertex as we did before, but this time in reverse.

Here is the algorithm to construct the inverse map. Start with the last vertex we added to  $I$ . If the current vertex was only negatively connected in the Seifert graph, then we use the map  $\varphi'_A$  to cap off the latest circle. If the vertex is both positively and negatively connected to the previous vertex, we use the map  $\varphi'_D$  to cap off the last circle. If the vertex is strictly positively connected, we use the map  $\varphi'_O$  to cap off the circle. For each map and stage of the composition, all other circles are mapped using the identity cobordism. We continue until we reach the last vertex, at which point we map using the identity cobordism.

**Proposition 4.2.5.** *The constructed  $I'$  is a chain map.*

*Proof.* By construction, similar to the map  $I$ , any vertex with a negative connection is removed using the map  $\varphi'_A$  or  $\varphi'_D$ . The compositions  $\varphi'_A \circ \Delta = 0$  and  $\varphi'_D \circ \Delta = 0$ . Since the image of the differential in the oriented resolution added is given purely by the image of split maps ( $\Delta$ ). Any such image will label two circles (which are negatively connected) with the same element. By observing the maps  $\varphi'_A$  and  $\varphi'_D$ , we see that two circles with the same label are killed by these maps. The only way an element could live would be to be an alternating state, alternating between  $a$  and  $b$  on adjacent circles. Again, since there are no odd cycles and all but one circle is removed by the map  $P$ , there must be a point in the composition where two circles with the same labeling are fed into either  $\varphi'_A$  or  $\varphi'_D$ . Hence, the image of any differential after composition with  $P$  will be 0. Thus  $I'$  is a chain map.  $\square$

**Proposition 4.2.6.** *The map  $I$  is invertible and  $I'$  is an inverse.*

*Proof.* The map  $P$  was constructed precisely to simplify with the map  $I$  using applications of the concertina-like relations of the type  $\varphi'_A \circ \varphi_A = -2\overline{Id}$ . If a vertex was only negatively connected, the circle was added in  $I$  by composition using the map  $\varphi_O$  and removed in  $P$  using the map  $\varphi'_A$ . From the list in the previous section we can see that this composition results in the map  $-Id$  on the circle which will be removed next. We use the maps  $\varphi'_A$  and  $\varphi'_D$  to remove the remaining circles. Note that the two maps  $\varphi'_A$  and  $\varphi'_D$  differ by a dot on either component. Using only the maps  $\varphi'_A$  and  $\varphi'_D$  guarantee that we construct a chain map, again by the no odd cycle property. Removing these maps in order will result in either  $-\overline{Id}$  a dotted identity or  $-2Id$ . So in all cases, undoing our composition results in either an identity or dotted identity. Hence the final resulting composition will be either the identity map or the dotted identity with powers of 2 present, all of which are invertible.  $\square$

The constructed inverse has a much higher degree than is necessarily needed to provide an inverse. Using similar constructions to  $I : C(U) \rightarrow C(D)$  and  $I' : C(D) \rightarrow C(U)$ , we can construct maps  $P : C(U) \rightarrow C(D)$  and  $P' : C(D) \rightarrow C(U)$  similarly. We construct  $P'$  using the maps  $\varphi'_A$  and  $\varphi'_O$  exactly as we constructed the map  $I$ , but with negatively connected vertices replacing positively connected ones.

**Proposition 4.2.7.** *The map  $P' : C(D) \rightarrow C(U)$  is a chain map which is an isomorphism on Lee homology.*

*Proof.* The proof is similar to the proofs that  $I$  is a chain map and mostly rely on the no odd cycle property of Seifert graphs. Any state in the image of a boundary map must have two identically labeled circles. Those circles will be killed by either the  $\varphi'_A$  or  $\varphi'_O$  maps. Looking at the definition of the maps  $\varphi'_A$  and  $\varphi'_O$ , we can see that if one feeds in the state which is alternately labeled with  $a$  and  $b$ , the image under  $I$  is non zero. The image of the map only depends on the label of the circle which is connected to the only circle in the unknot diagram. The image thus contains both  $a$  and  $b$  and is seen to be an isomorphism.  $\square$

The names  $I$  and  $P$  chosen in this section are meant to imply injection and projection, referring to the maps direction relative to the unknot. One map injects the chain complex of the unknot, the other projects the more complicated diagram to that of the unknot.

### 4.3 Bounds on Rasmussen's Invariant

In this section we begin by introducing some notation regarding Seifert graphs which will allow us to more easily determine the degrees of the resulting maps from the previous section. Let  $\Gamma$  be a graph. Let  $e(\Gamma)$  be the number of edges present in the graph. Let  $v(\Gamma)$  be the number of vertices. Let  $c(\Gamma)$  be the number of components of the graph.

These descriptions and the construction of the map  $I$  in the previous section give us an easy way to determine the degree of the final composition.

**Proposition 4.3.1.** *Given the diagram  $D$  of a knot  $K$ , the map  $I : \mathcal{H}_{Lee}(U) \rightarrow \mathcal{H}_{Lee}(D)$  has filtration degree  $w(D) - v(T(D)) + 2c(T^+(D)) - 1$ .*

*Proof.* We constructed the map  $I$  using compositions of the maps  $\varphi_A$  and  $\varphi_O$ . These maps have degree  $-1$  and  $+1$  respectively. We used the map  $\varphi_A$  to add each positively connected circle beyond the first in each connected component of the diagram. Thus the composition regarding the negative circles provides  $v(T(D)) - c(T^+(D))$  (this accounts for all vertices except for the first chosen vertex and the first vertex of each component after that) compositions of degree  $-1$  resulting in the  $v(T(D))$  terms in the degree calculation. The vertices which were added at the beginning of each component of the graph were added using the degree 1 map,  $\varphi_O$ , a total of  $c(T^+(D)) - 1$  times (all but the first circle). The total degree (which is additive under composition) is  $w(D) - v(T(D)) + 2c(T^+(D)) - 1$ . The writhe shift is present due to the fact that we are using normalized Khovanov homology and the fact that the writhe of an untwisted unknot is 0.  $\square$

Note that this bound does not depend on the choice of spanning forest above, only on the number of times each map was used. Thus the bound is independent of the choices (other than diagram) which were made to construct the map  $I$ . This proposition allows us to give a lower bound on Rasmussen's invariant for any knot, which depends on the given diagram of the knot.

**Theorem 4.3.2.** *For a knot  $K$  and a diagram  $D$  of  $K$  we obtain the lower bound*

$$s(K) \geq w(D) - v(T(D)) + 2c(T^+(D)) - 1$$

*Proof.* This follows from the degree of the constructed  $I$  and the fact that the  $s$  invariant of the unknot is 0.  $\square$

We can see immediately that for a positive diagram  $D$  (a diagram with no negative crossings) of a knot  $K$  that this bound agrees with the known fact  $s(K) = w(D) - v(T(D)) + 2c(T^+(D)) - 1 = n_+ - v(T(D)) + 1$  for positive diagrams. Thus, strictly negative circles present in the diagram give us a way to increase the lower bound for the  $s$  invariant.

We also obtain upper bounds using the map  $P'$ .

**Proposition 4.3.3.** *Given the diagram  $D$  of a knot  $K$ , the map  $P' : \mathcal{H}_{Lee}(D) \rightarrow \mathcal{H}_{Lee}(U)$  has filtration degree  $-w(D) - v(T(D)) + 2c(T^-(D)) + 1$*

**Theorem 4.3.4.** *For a knot  $K$  and a diagram  $D$  of  $K$  we obtain the upper bound*

$$s(K) \leq w(D) + v(T(D)) - 2c(T^-(D)) + 1$$

So, we can see that, given a diagram, we obtain bounds on the  $s$  invariant (and hence lower bounds on the slice genus) just by looking at the connectivity of circles in the Seifert graph. Thus we get the bounds

$$w(D) - v(T(D)) + 2c(T^+(D)) - 1 \leq s(K) \leq w(D) + v(T(D)) - 2c(T^-(D)) + 1$$

These bounds show that the  $s$  invariant is bounded from the writhe by the number of circles in the Seifert resolution, hence, the smaller the number of circles in the resolution, the better the bound. These bound also show that a circle with only positive connections will decrease the upper bound and a circle with only negative connections will increase the lower bound. From these results and the relationship of the  $s$ -invariant with the slice genus, we get the following bound

$$2g_4(K) \geq w(D) - v(T(D)) + 2c(T^+(D)) - 1$$

for any diagram  $D$  of the knot  $K$ .

We can also investigate the difference in these upper and lower bounds to determine when these bounds are in fact equal. The difference,  $\Delta_s(D)$ ,

$$\begin{aligned} & (w(D) + v(T(D)) - 2c(T^-(D)) - 1) - (w(D) - v(T(D)) + 2c(T^+(D)) - 1) \\ &= 2v(T(D)) - 2c(T^-(D)) - 2c(T^+(D)) + 2 \\ &= 2[v(T(D)) - c(T^-(D)) - c(T^+(D)) + 1] \end{aligned}$$

is given by  $2[v(T(D)) - c(T^-(D)) - c(T^+(D)) + 1]$ . This shows that the bounds are in fact equal when this quantity is zero. Examining this calculation, we can determine when this difference will be zero. The difference in the bounds is 0 for positive knot diagrams as  $c(T^-(D)) = v(T(D))$  and  $c(T^+(D)) = 1$ . Similarly for negative knots diagrams. But this difference is also 0 for alternating knot diagrams. If a knot has an alternating diagram, the oriented resolution, and thus the Seifert graph has a special property. The complement of the oriented resolution of an alternating diagram can be separated into two regions, one positive and one negative, such that adjacent regions have opposite signs. These regions are labeled so that any positive crossing appears in the positive region and each negative crossing appears in each negative region. Each region contributes a component to either  $c(T^-(D))$  or  $c(T^+(D))$ . There is one more region than there are circles in the oriented resolution, so  $v(T(D)) + 1 = c(T^-(D)) + c(T^+(D))$ . Thus we can see that the difference between the bounds must be 0.

Another class of knots for which the two bounds agree are closures of homogeneous braids. A homogeneous braid is a braid that can be written as a word where either  $\sigma_i$  or  $\sigma_i^{-1}$  appears, but not both. The corresponding Seifert graph of the closure of the braid is easily seen to be a straight line with a vertex for each circle in the oriented resolution. Each set of edges between a vertex have the same sign, so each edge decreases the number of components of either  $T^+(D)$  or  $T^-(D)$ , but not both. There is one less edge than vertex, so there are a total of  $n + 1$  components. Thus the difference between the bounds is 0.

Thanks to the work of Abe in [Abe10], we have the following characterization of knots for which this bound is tight. A cut vertex is a vertex where, if removed from the original graph, the resulting graph has more components. A block of a graph is a maximal subgraph with no cut vertices. A signed graph is homogeneous if each block has the same sign. We say a link is homogeneous if it has a homogeneous diagram.

**Theorem 4.3.5.** [Abe10] *A diagram  $D$  of a knot is homogeneous if and only if  $\Delta_s(D) = 0$*

So this class of knot diagram is exactly the class for which our bounds are tight. This class of knot includes alternating knots, positive and negative knots, as well as homogeneous braids. There are knots which are homogeneous but not alternating,

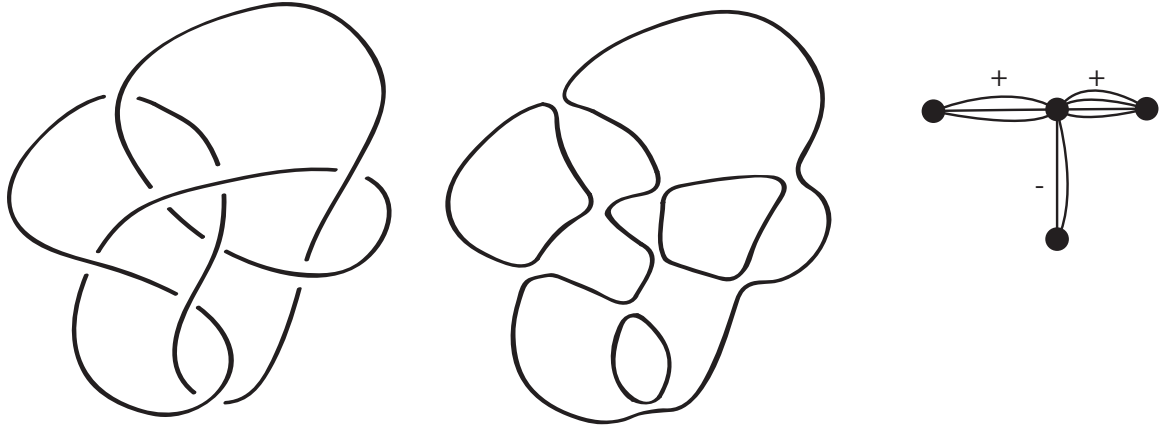


Figure 4.6: A homogeneous diagram of the knot  $9_{43}$

nor positive. The knot  $9_{43}$  in the knot table shown in figure 4.6 is the simplest knot which is homogeneous but neither alternating nor positive.

## 4.4 Representative Cycles

In the previous section, we constructed bounds on the  $s$ -invariant which are easy to compute just by diagrammatic calculations. The formalism allows us to obtain precise representatives of the homology classes whose filtration degrees we need to compute if we are to get an exact value of  $s$ . A note about these states, since we showed that the map can be constructed using the  $\varphi_O$  map on strictly negative components, we can determine that there is a state representing Lee homology classes with 1 labels on all strictly negatively connected circles. The labellings on the other circles depend on the choice of spanning trees in the construction of  $I$ . The difference being which positive component was chosen first. This component will have different labellings dependent on whether a 1 is fed into the constructed map or an  $x$ . The labellings on all positive patches are given by linear combinations of the basis elements  $a$  and  $b$  and can be worked out for any given choice. The chain maps which provide an upper bound for the  $s$  invariant do not construct a representative cycle. If it did, all  $s$ -invariants would be determined by this bound, as the  $s$ -invariant is defined by the highest filtration degree of the cycles which represent it. It is easy to find examples where the constructed upper bound does not agree with the actual  $s$ -invariant of the knot. We now discuss the image of the constructed map  $I$ . To do this, we will first

consider, for a positive diagram  $D$ , the elements of  $\mathcal{H}_{Lee}(D)$  which represent the Lee homology. The degree of the Lee generators of a positive diagram are known to be  $n_+ - v(T(D)) + 1 \pm 1$ . The generators are given by  $s_o \pm s_{\bar{o}}$ . The states  $s_o$  and  $s_{\bar{o}}$  are given by labellings of circles by alternating  $a$ 's and  $b$ 's in the oriented resolution. In our chosen basis representatives,  $a = 1 + x$  and  $b = 1 - x$ , we can see that these states resemble the following

$$a \otimes b \otimes a \otimes \cdots \otimes b \otimes a$$

and

$$b \otimes a \otimes b \otimes \cdots \otimes a \otimes b$$

Expanding these in terms of the  $1, x$  basis we obtain

$$(1 + x) \otimes (1 - x) \otimes (1 + x) \otimes \cdots \otimes (1 - x) \otimes (1 + x)$$

and

$$(1 - x) \otimes (1 + x) \otimes (1 - x) \otimes \cdots \otimes (1 + x) \otimes (1 - x)$$

We can further expand these using the properties of tensor products. We will collect terms with like degrees

$$\begin{aligned} & 1 \otimes 1 \otimes \cdots \otimes 1 \\ & x \otimes 1 \otimes 1 \otimes \cdots \otimes 1 - 1 \otimes x \otimes 1 \otimes \cdots \otimes 1 \cdots + 1 \otimes 1 \otimes \cdots \otimes 1 \otimes x \\ & \quad \vdots \\ & 1 \otimes x \otimes x \otimes \cdots \otimes x - x \otimes 1 \otimes x \otimes \cdots \otimes x \cdots + x \otimes x \otimes \cdots \otimes x \otimes 1 \\ & \quad x \otimes x \otimes \cdots \otimes x \end{aligned}$$

The signs present on each term can be determined by examining which circles have a label  $b$  and determining the number of  $x$ 's in the term contributed by such circles. This shows that there is parity involved in the signs of each individual term, but one can see that changing between the  $s_o$  and  $s_{\bar{o}}$  labellings will change the sign of each term in a predictable fashion. So, terms which have an even number of  $x$ 's contributed from  $b$  labeled circles are positive, while terms with an odd number of  $x$ 's contributed from  $b$  labeled circles are negative. We are interested in the terms which contribute to lower quantum gradings, so we will now look at the sign of the all  $x$  term. To do this we must consider the parity of the number of circles in the oriented resolution. Once

again, the Seifert graph is bipartite, meaning the circles in the oriented resolution can be separated into two groups. This separation is determined by the induced orientation on the resolution. If the number of circles oriented clockwise has the same parity as the number of circles oriented counter-clockwise, then the all  $x$  term will have the same sign in both  $s_o$  and  $s_{\bar{o}}$ . If the number of circles in each group have differing parity, one of the labellings will have an odd number of  $b$ 's, the other an even number. So the all  $x$  terms in this case will have differing signs. We get the following classification

**Proposition 4.4.1.** *The states  $s_o \pm s_{\bar{o}}$  lie in different quantum filtration gradings. If the number of clockwise oriented circles in the oriented resolution has the same parity as the number of counter-clockwise oriented circles, then  $s_o \pm s_{\bar{o}}$  lives in grading  $n_+ - v(T(D)) + 1 \pm 1$ . Otherwise,  $s_o \pm s_{\bar{o}}$  lives in grading  $n_+ - v(T(D)) + 1 \mp 1$ .*

More can be said about these particular states. Each term in  $s_o \pm s_{\bar{o}}$  has congruent quantum grading mod 4. This gives us an easy way to determine the representatives combinatorially. We simply need to express all terms with a given number of  $x$ 's and 1's with the appropriate signs, which are forced due to alternate labellings of adjacent circles. So,  $s_o \pm s_{\bar{o}}$  is generated given by all terms with an even number of  $x$ 's (with appropriate signs) and  $s_o \mp s_{\bar{o}}$  is given by all terms with an odd number of  $x$ 's.

Now back to the maps we used to create our bounds. The image of this map is the alternate labeling of circles by  $a$ 's and  $b$ 's. Thus the image of our map is the two states  $s_o$  and  $s_{\bar{o}}$ . Thus their sum and difference is in the image as well. In fact, the image of 1 under the given map will always be the higher of the two quantum gradings, for degree reasons. We can see this also by the fact that if we feed a 1 into the map, that the all  $x$  term does not appear. So, the image of 1 under the constructed map is given by the sum of terms with an appropriate number of  $x$ 's and signs based on the parity of the number of circles in the oriented resolution.

We now combine this information about positive diagrams with the general construction of our map. The constructed map simply copies this idea to each connected component. The exception being components with only one vertex, which simply get the labeling of 1 in the resulting state. So the image of the map is the tensor product of the above states for each connected component of the graph. The signs are determined by the connectivity of the graph and the parity of each connected



component.

We conclude this section with an example. The maps for the  $4_1$  knot given in figure 4.5 will yield the following states. When we feed the state 1 into the map, the output is given by  $x \otimes 1 \otimes 1 - 1 \otimes x \otimes 1$ . Feeding in the state  $x$  results in the output  $1 \otimes 1 \otimes 1 - x \otimes x \otimes 1$  (thanks to the fact that  $x^2 = 1$ ). These two states have quantum gradings  $-1 + 1 + 1 = 1$  and  $-1 - 1 + 1 = -1$ , respectively, giving a lower bound of  $0 \leq s(4_1)$ . Since the diagram is alternating and hence homogeneous, Abe's theorem indicates that the  $s$  invariant for this knot is 0 and the Lee homology is realized by those states.

# Chapter 5

## Positive Braids and Thickness

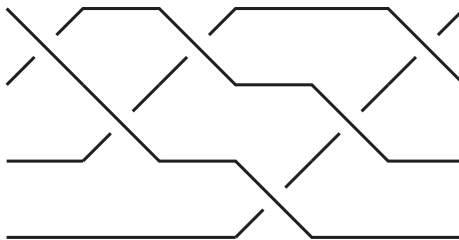
In this chapter we show that the homological thickness of (the closure of) a positive braid is related to the Garside index of the braid. This gives more positive evidence toward one of Khovanov's conjectures stated in [Kho03]. His conjecture states that all prime braid-positive knots other than the  $T(2, 2k + 1)$  torus knots are Khovanov thick. In [Sto07], Stosic showed that all other torus knots are thick. We widen the class of braid-positive knots which are thick to braids which have a torus-like twist anywhere in their presentation. This class also includes all known thick torus knots.

### 5.1 Garside Powers and Thickness

There are many useful classes of knot diagrams in knot theory: alternating diagrams, quasi-alternating, and as seen in the last chapter, homogeneous diagrams. We now discuss another relevant type of diagram, this time for braid-positive links. The key element in our thickness result is a normal form presented by Garside as a solution to the word problem for positive braids. For each  $n \in \mathbb{Z}$ , the braid group  $B_n$  has a special element  $\Delta_n$  called the Garside element. This element can be written

$$\Delta_n = (\sigma_1)(\sigma_2\sigma_1) \dots (\sigma_{n-1} \dots \sigma_1).$$

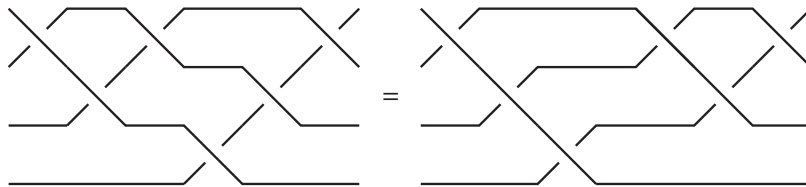
Illustrated below is  $\Delta_4$ , an element of  $B_4$



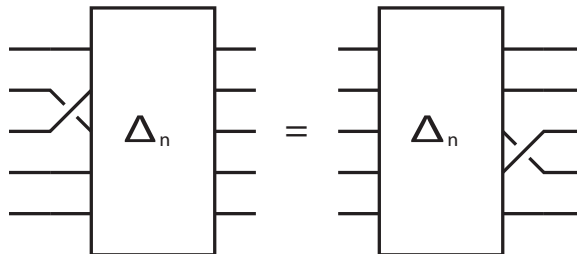
These elements can also be described inductively, using the natural inclusion of braid groups  $B_n \hookrightarrow B_{n+1}$  where we include a braid on the first  $n$  strands. We can describe  $\Delta_n$  as

$$\Delta_n = \Delta_{n-1}(\sigma_{n-1} \cdots \sigma_1)$$

We, again, illustrate this with our 4 strand example



The Garside element is also known as a half twist. The half twist has the following commutation relation  $\Delta_n \sigma_i = \sigma_{n-i} \Delta_n$ . Thus a full twist,  $\Delta_n^2$ , commutes with each generator  $\sigma_i$  and hence each braid. The full twist  $\Delta_n$  generates the center of the braid group  $B_n$ .



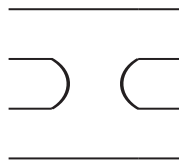
Each braid, whether positive or not, has a special form called the Garside normal form.

**Proposition 5.1.1** (Garside). *Any braid  $b \in B_n$  can be written in the form  $\Delta_n^k b^+$  where  $k \in \mathbb{Z}$  and  $b^+ \in B_n^+$ .*

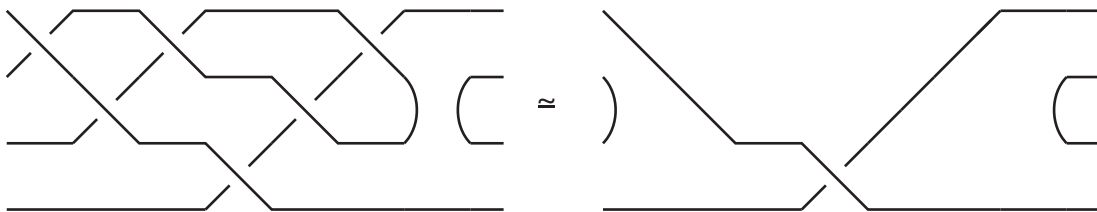
*Proof.* We can replace the inverses of the generators,  $\sigma_i^{-1}$ , with a conjugate braid of the form  $\Delta_n^{-1} b_i^+$  for some  $b_i^+ \in B_n^+$  (One writes  $\Delta_n^{-1} \Delta_n$  and omits one positive exponent to do so). We can then collect all of the powers of  $\Delta_n$  on the left using the commutation relations. The resulting braid is of the desired form as the commutation relations do not change the exponents of the  $\sigma_i$  □

By pulling out powers of  $\Delta_n$  from  $b^+$  and using cancellations of the form  $\Delta_n \Delta_n^{-1} = Id$ , one obtains a minimal presentation of the form  $\Delta_n^k b^+$  where  $b^+$  has no factors of  $\Delta_n$ . We call  $k$ , the the exponent of the Garside element in the minimal presentation, the Garside index of the braid. Note that  $k$  can be positive or negative. In the case of positive knots,  $k \geq 0$ .

We will now outline some facts about this special element of the braid group as it relates to links. The primary fact we will make use of is that in the given presentation of the half twist, each strand crosses each other strand once and only once. With the standard orientation of the braid, each of the crossings in the half twist is positive. We will be considering the Khovanov complex of positive braids, so we must consider what happens to the braids when a plat (that is to say the unoriented resolution of a positive crossing) is placed beside a half twist. A plat is a braid like element of the following form



Plats are described as turn-backs and are not elements of the braid group, but are necessary objects when studying links as braid closures. Let  $e_i$  represent the plat which connects strand  $i$  to strand  $i + 1$ . The Garside element behaves very well with regards to turn-backs. When a plat is placed adjacent to a Garside element, the plat can be “pulled” through the braid element to the beginning of the link element. The plat also remains connected to the two strands it was connected to at the end of the Garside element once pulled through the diagram. This reduction in the number and type of crossings will be useful in computing the homology of certain links via the long exact sequences.



When given the standard orientation, the Garside element  $\Delta_n$  has  $n(n - 1)/2$  crossings, each of which is positive. We now give a count of negative crossings when a plat placed next to a Garside element. The presence of the plat means we cannot

give the braid the standard orientation.

**Lemma 5.1.2.** *Let  $b = \Delta_n e_i b'$  be a generalized braid element with  $b, b' \in B_n$ . The link formed by the closure of  $b$  will have at least  $n - 1$  negative crossings, regardless of orientation.*

*Proof.* We inspect the standard presentation of the Garside element for this result. Give the resulting braid any orientation. Due to the plat, the two strands connected by the plat must have opposite orientation. Each strand in the Garside element crosses each other strand exactly once. Therefore, one of the plat connected strands must produce a negative crossing with each other strand in the braid, of which there are  $n - 2$ . The plat strands also cross each other, providing the  $n - 1$ st negative crossing.  $\square$

Since a plat can pull through a Garside element and the result is a plat on the same two strands, a plat can be pulled through multiple adjacent Garside elements.

**Proposition 5.1.3.** *A power of the Garside element  $\Delta_n^k$  with  $k \geq 0$  adjacent to a plat has at least  $k(n - 1)$  negative crossings, each of which can be removed by isotopy.*

*Proof.* Each copy of the Garside element has two strands which ultimately connect to the plat, giving them opposite orientation. Thus the lemma above provides the  $n - 1$  negative crossings for each power of the Garside element. The plat can be pulled through each copy and thus can be isotoped out of the diagram.  $\square$

The skein long exact sequence in Khovanov homology behaves well with the ability to pull plats through the half twist. It allows us to show that positive crossings which occur adjacent to the half twist have no effect on the homology groups in low homological dimensions. First, a lemma regarding the homology of an unshifted complex.

**Lemma 5.1.4.** *If a diagram  $D$  can be isotoped to a diagram  $D'$  with  $l$  fewer negative crossings, then  $H^i(D) = 0$  for all  $i < l$ .*

*Proof.* Let  $n_- = n_-(D)$  and  $n'_- = n_-(D')$ . Then  $l = n_- - n'_-$ . By prop. 3.3.1,  $\mathcal{H}(D')^i = 0$  for each  $i < n'_-$ . So  $\mathcal{H}(D)^i = 0$  for  $i < n'_-$  as these diagrams represent the same link. Thus  $H(D)^i = 0$  for  $i < l$ .  $\square$

With this assertion, we can prove the following.

**Lemma 5.1.5.** *Let  $b \in B_n^+$ . Let  $b_1 = \Delta_n^k b$  and  $b_2 = \Delta_n^k \sigma_j b$  for any  $1 \leq j \leq n-1$  and  $k \geq 0$ . Then*

$$H^{i,q}(b_1) = H^{i,q+1}(b_2) \text{ for } i \leq k(n-1)$$

*Proof.* We use the long exact sequence for a distinguished positive crossing, that crossing being  $\sigma_j$ . The crossing is positive and thus we use the positive crossing long exact sequence

$$\begin{aligned} \rightarrow H^{i-1,j-1}(K_1) \rightarrow H^{i,j}(K) \rightarrow H^{i,j}(K_0) \rightarrow \\ \rightarrow H^{i,j-1}(K_1) \rightarrow H^{i+1,j}(K) \rightarrow H^{i+1,j}(K_0) \rightarrow . \end{aligned}$$

Since the unoriented resolution  $K_1$  features a plat adjacent to a Garside element, we know that the chain complex corresponding to  $K_1$  is homotopy equivalent to one with  $n-1$  fewer negative crossings. Hence  $H^{i,j}(K_1) = 0$  for all  $i < n-1$ . This means, that for such  $i < n-1$ , the long exact sequence reduces to

$$\rightarrow 0 \rightarrow H^{i,j}(K) \rightarrow H^{i,j}(K_0) \rightarrow 0$$

showing that the unshifted homological groups of  $K$  and  $K_0$  are isomorphic for  $i < n-1$ . We can use the fact that  $k(n-1)$  crossings are removable to establish this fact for higher powers of the Garside element.  $\square$

So, we can add crossings to a positive braid presentation containing a half twist while preserving low homological dimension. We will use this observation to establish thickness of positive braids with certain Garside normal form. The method of proof we use to establish thickness follows that of Stosic. The following result is from [Sto07], where he established the thickness of torus knots.

**Theorem 5.1.6.** *(Stosic) Let  $K = T_{p,q}$ ,  $3 \leq p \leq q \in \mathbb{Z}$  be a torus link. Then*

$$\text{rank } \mathcal{H}^{4,(p-1)(q-1)+5}(T_{p,q}) > 0$$

This fact, that the fourth homology group is nontrivial in the given quantum grading, provides the required thickness. This gives us an element on the  $j - 2i = (p-1)(q-1) + 5 - 2(4) = (p-1)(q-1) - 3$  diagonal. Two other diagonals are provided by the fact that the  $s$ -invariant of a positive braid has quantum grading

$(p-1)(q-1)$ , so the corresponding homological representatives lie in quantum grading  $(p-1)(q-1) \pm 1$ . We then have that the homology of the  $(p, q)$  torus knot occupies at least three diagonals and are thus Kh-thick. This result shows that not only are most torus knots Kh-thick, but that the thickness occurs in low homological dimension. We will establish a similar fact for many braid positive links using the Garside normal form. This will allow us to extend the thickness results to any braid with a relatively low Garside index.

We begin by calculating the Khovanov homology of the closure of the Garside braid. Note that the Garside braids are defined inductively and the closure of  $\Delta_n$  relates to  $\Delta_{n+1}$  quite nicely. In the given presentation of the Garside element  $\Delta_{n+1}$ , only one power of  $\sigma_n$  is present. Therefore, in the closure of the braid, this crossing is simply a Markov stabilization and can be removed without affecting the closure type of the braid. The result will be a braid whose closure is given by  $\Delta_n$  with a few extra positive crossings. As we have seen above, those crossings can be removed to show that the first few homology groups are in fact the same for  $\Delta_{n+1}$  and  $\Delta_n$ .

**Proposition 5.1.7.** *For the closures of the Garside elements  $\Delta_{n+1}$  and  $\Delta_n$ , we have*

$$\mathcal{H}^{i,j+n-1}(\Delta_{n+1}) = \mathcal{H}^{i,j}(\Delta_n) \text{ for } i \leq n-1$$

*Proof.* Since  $\Delta_{n+1} = \sigma_n \cdots \sigma_1 \Delta_n$  we can compare their respective closures. The closure of  $\sigma_{n-1} \cdots \sigma_1 \Delta_n$  on  $n$  strands is the same link as the closure of  $\Delta_{n+1}$  so their homology groups agree. The braid  $\sigma_{n-1} \cdots \sigma_1 \Delta_n$  is conjugate to  $\Delta_n \sigma_{n-1} \cdots \sigma_1$ , so they have the same closure. We can then use the above lemma to remove each  $\sigma$  on the right of the  $\Delta_n$ .  $\square$

We will now establish the thickness of the closure of the Garside element for small  $n$  by presenting the corresponding Poincaré polynomials in table 5.1. The Poincaré polynomials are too large for the table, so they are truncated after the fourth homological degree. The thickness of their respective homologies is established by that point. The table also shows stability (after a quantum grading shift of  $n-2$ ) of the first homology groups for each of the closures. We can see that for  $n \geq 5$ , the closures of the Garside delta braids are indeed thick. We can also see that the squares of Garside delta braids are also Kh-thick for  $n \geq 3$ .

Table 5.1: Thickness of Garside Braid  $(\Delta_n)$  Closures

n	Poincaré Polynomial	S = { 2i - j }
2	$\mathbf{q}^{-1} + \mathbf{q}$	{-1, 1}
3	$\mathbf{1} + \mathbf{q}^2 + q^4t^2 + q^6t^2$	{0, 2}
4	$\mathbf{q}^2 + \mathbf{q}^4 + q^6t^2 + q^{10}t^3 + q^{10}t^4 + q^{12}t^4$	{2, 4}
5	$\mathbf{q}^5 + \mathbf{q}^7 + q^9t^2 + q^{13}t^3 + \mathbf{q}^{11}t^4 + 2q^{13}t^4 + \dots$	{3, 5, 7}
6	$\mathbf{q}^9 + \mathbf{q}^{11} + q^{13}t^2 + q^{17}t^3 + \mathbf{q}^{15}t^4 + q^{17}t^4 + \dots$	{5, 7, 9, 11}
7	$\mathbf{q}^{14} + \mathbf{q}^{16} + q^{18}t^2 + q^{22}t^3 + \mathbf{q}^{20}t^4 + q^{22}t^4 + \dots$	{8, 10, 12, 14, 16}
8	$\mathbf{q}^{20} + \mathbf{q}^{22} + q^{24}t^2 + q^{28}t^3 + \mathbf{q}^{26}t^4 + q^{28}t^4 + \dots$	{12, 14, 16, 18, 20, 22}
9	$\mathbf{q}^{27} + \mathbf{q}^{29} + q^{31}t^2 + q^{35}t^3 + \mathbf{q}^{33}t^4 + q^{35}t^4 + \dots$	{15, 17, 19, 21, 23, 25, 27, 29}

Table 5.2: Thickness of squares of Garside Braid  $(\Delta_n^2)$  Closures

n	Poincaré Polynomial	S = { 2i - j }
2	$\mathbf{1} + \mathbf{q}^2 + q^4t^2 + q^6t^2$	{0, 2}
3	$\mathbf{q}^3 + \mathbf{q}^5 + q^7t^2 + q^{11}t^3 + \mathbf{q}^9t^4 + 3q^{11}t^4 + 2q^{13}t^4$	{1, 3, 5}
4	$\mathbf{q}^8 + \mathbf{q}^{10} + q^{12}t^2 + q^{16}t^3 + \mathbf{q}^{14}t^4 + q^{16}t^4 + \dots$	{4, 6, 8, 10}
5	$\mathbf{q}^{15} + \mathbf{q}^{17} + q^{19}t^2 + q^{23}t^3 + \mathbf{q}^{21}t^4 + q^{23}t^4 + \dots$	{7, 9, 11, 13, 15, 17}
6	$\mathbf{q}^{24} + \mathbf{q}^{26} + q^{28}t^2 + q^{32}t^3 + \mathbf{q}^{30}t^4 + q^{32}t^4 + \dots$	{12, 14, 16, 18, 20, 22, 24, 26}



These lemmas establish the following facts. If a positive braid has a high enough Garside power relative to its braid index, then the knot is Kh-thick. To put it precisely,

**Theorem 5.1.8.** *Let  $b \in B_n^+$  be a positive braid. Let  $b = \Delta_n^k b^+$  be the Garside normal form of the braid. If  $n \geq 3$  and  $k \geq 2$  or if  $n \geq 5$  and  $k \geq 1$ , then the link formed by the closure of  $b$  is Kh-thick.*

*Proof.* We apply the above lemma to remove each positive crossing in  $b^+$ . The thickness of a Garside braid appears in homological degree 4, so all that is required is  $(k)(n-1) > 4$ . This occurs when  $n \geq 5$  and  $k \geq 1$  or when  $n \geq 3$  and  $k \geq 2$ . The closure of the braid then has the same first four homology groups as the corresponding Garside Power (up to some positive quantum grading shift), and the Kh-thickness is present.  $\square$

Thus we obtain many Kh-thick knots. A result of Sullivan [Sul97] states that positive braids with a half twist, whose closures are knots, are prime. Thus we can create thick knots by starting with Garside powers and closing the positive braid to a knot. This result reestablishes the fact that the torus knots  $T(p, q)$  for  $p, q \geq 3$  are thick as the  $T(p, q)$  torus knot ( $p < q$ ) can be obtained as the closure of the braid  $\Delta_p^2 b$  for some positive braid  $b \in B_p$ .

# Chapter 6

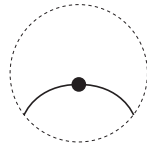
## Injectivity of Homology of Certain Links

In this chapter we will show that under certain conditions, cobordisms will help us determine the homology groups of certain links. The question we ask is what kind of homological comparisons can we get using cobordisms. In general, a cobordism with high genus will destroy much of the homology present, simply for degree reasons. It is because of this that we restrict our studies to cobordisms with low genus.

### 6.1 The Reidemeister Invariance Maps

In Dror Bar-Natan's paper [BN05], he gives geometric descriptions of the maps which correspond to the Reidemeister moves. These maps and their inverses show that two complexes which differ by a Reidemeister move have homotopy equivalent chain complexes. We will make extensive use of these maps and their properties in the next section. The key step in these relations is the behavior of a merge followed immediately by a split. This composition will result in a tube connecting each of the original components. First we need a way to describe our chain maps diagrammatically. As in chapter 4, the dotted surface represents one half of the related surface with genus.

**Proposition 6.1.1.** *Let  $D$  be a link diagram. The map given by*

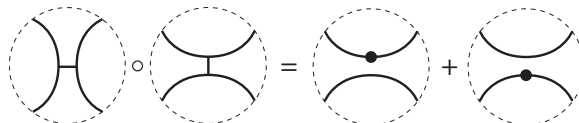


*on one component and identities elsewhere is a chain map from  $C(D)$  to itself.*

*Proof.* Call this map  $f : C(D) \rightarrow C(D)$ . What we show here is that functorial cobordisms between knots are in fact maps of  $A$ -modules. The map  $f$  is the identity on all components but the marked one, so we must investigate how the dotted piece interacts with each part of the differential. The dot acts by multiplication by  $x$  on the appropriate tensor factor of  $A$ . The differential corresponding to the dotted piece can either be an identity, split or merge. In any of these cases, the action of the dot commutes with the differential.  $\square$

We can therefore describe a self chain map on a complex  $C(D)$  by a dotted diagram of the link. The dot indicates which component to place the one half saddle in the resulting chain map.

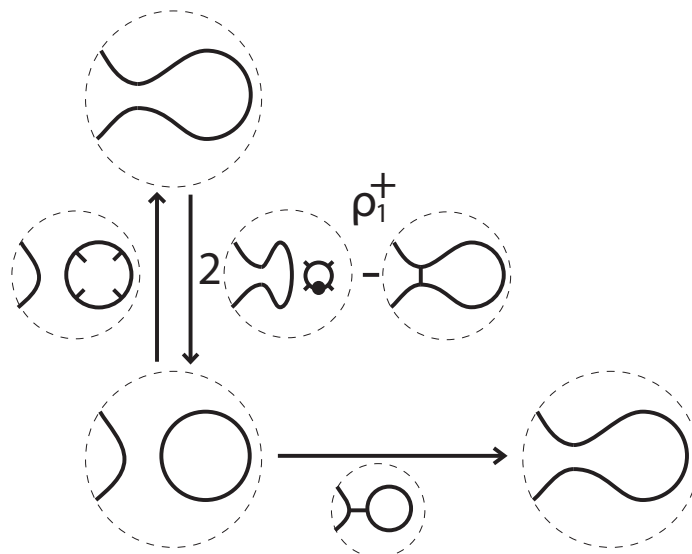
Using the neck cutting relation, we get the following relationship:



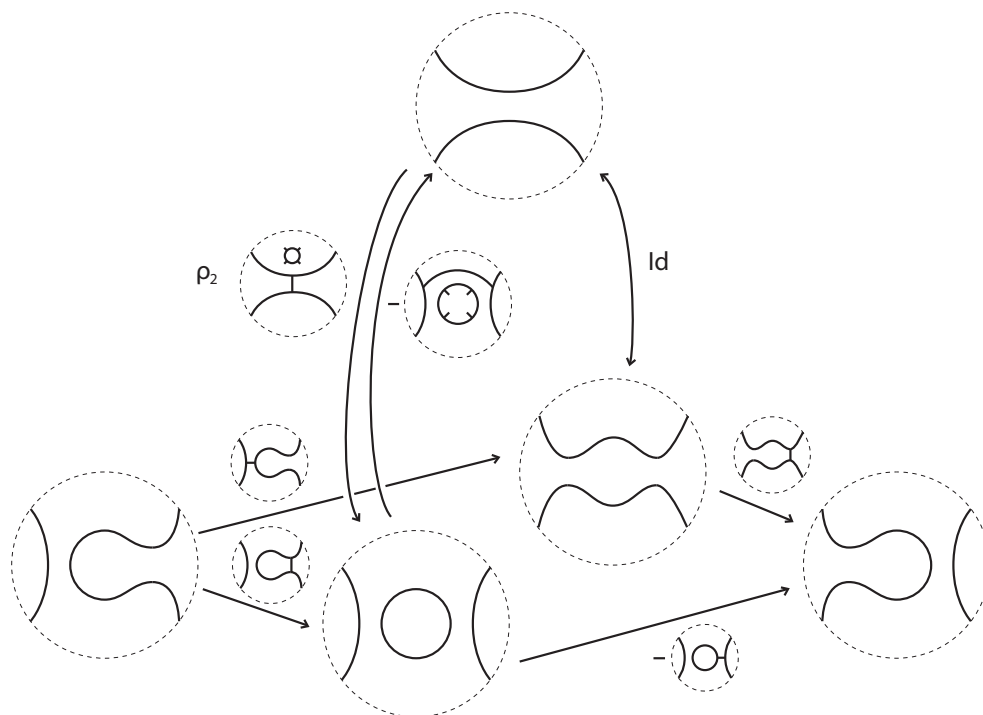
The composition of two saddles results in a tube. Using the neck cutting relation on this tube, we can see that the resulting morphism is a sum of other maps. These two maps are each dotted identity maps, one term for each side of the merged components.

We will adopt the following naming convention for these maps. We will not be using the Reidemeister three move. In the case of Reidemeister moves one and two, one of the two related diagrams has more crossings. Our naming will be such that  $\rho_1$  and  $\rho_2$  map to the diagram with more crossings. The maps the other direction will be designated with a prime,  $\rho'_1$  and  $\rho'_2$ . Finally, the diagram with an extra crossing in the Reidemeister one move will differ by having either extra negative crossings or positive crossing. We denote these (when appropriate) by a superscript plus or minus. For example, the map  $\rho'_1$  is the map from the diagram with an extra positive loop to the diagram without.

We present these cobordisms here for reference. First,  $\rho_1^+$ , the Reidemeister I move for a positive crossing



Second,  $\rho_2$ , the second Reidemeister move



The following are the chain maps themselves, without the complexes present for clarification

$$\rho_1^+ = 2 \left( \text{Diagram 1} \right) - \left( \text{Diagram 2} \right)$$

$$\rho_2 = \left( \text{Diagram 3} \right) \oplus \left( \text{Diagram 4} \right)$$

The main technique we will use will be to compose an invariance map with its inverse. In the proof that the chain complexes are indeed homotopy equivalent, one uses a chain homotopy  $h$ . The terms of this homotopy are zero in the compositions we are interested, namely the compositions  $\rho'_1 \circ \rho_1$  and  $\rho'_2 \circ \rho_2$ . One can easily check that these compositions all result in the identity map on the components involved. For our purposes, the maps will also be decorated with dots. So we must investigate how the maps behave under the presence of dots, that is what does the composition  $\rho'_1 \circ f \circ \rho_1$  look like, where  $f$  is an identity map with a dotted component. We investigate the composition of the first Reidemeister map with dotted identities.

$$\left( \text{Diagram 1} \right) \circ \left( \text{Diagram 2} \right) \circ 2 \left( \text{Diagram 3} \right) - \left( \text{Diagram 4} \right) = - \left( \text{Diagram 5} \right)$$

This composition shows that if we twist a strand, compose with a dotted identity, then untwist the strand, the result is again a dotted identity (with an overall negative sign). So the dot anticommutes with a Reidemeister I move. The resulting composition is similar for a negatively twisted Reidemeister I move. For the second Reidemeister move,

$$\begin{aligned} & - \left( \text{Diagram 1} \right) + \left( \text{Diagram 2} \right) \circ \left( \text{Diagram 3} \right) \oplus \left( \text{Diagram 4} \right) \circ \left( \text{Diagram 5} \right) \oplus \left( \text{Diagram 6} \right) \\ & = \left( \text{Diagram 7} \right) - \left( \text{Diagram 8} \right) - \left( \text{Diagram 9} \right) = - \left( \text{Diagram 10} \right) \end{aligned}$$

The action of the dot on the other strand in the Reidemeister two move can be determined from symmetry. So, what this shows is that under composition with a dot, the dot remains in the Reidemeister one type moves and “pulls through” the Reidemeister two moves. Again, overall signs appear, but signs can be inverted. It is

also clear, given the local nature of these moves, that a dot located away from these moves remains at its original location. These maps lay the groundwork for the next section. We will repeatedly use these maps to determine the relationship between the homology of diagrams related in specific ways. What we have shown is that the action of dotted cobordism (up to overall sign) commutes with Reidemeister move maps.

## 6.2 Injectivity Result

In this section we describe the construction of diagrams which will ultimately have related homology. The actions we describe will be called “ribbon moves”. We will essentially pull ribbon like pieces of link diagrams using Reidemeister moves to obtain related diagrams. The prototype example will be the one in figure 6.1, showing a relationship between a diagram of the unknot and a diagram of the knot  $6_1$ . We will consider changes between diagrams which are isotopies and Reidemeister moves of type one and two. Reidemeister III will be unnecessary in these constructions. We may always assume that the ribbon is “thin” enough to avoid needing the triple point move. Pulling the ribbon past a double point can be accomplished using two sequential Reidemeister II moves near the crossing instead. The ultimate goal is to construct an identity cobordism from a diagram to itself which factors through the homology associated to another knot diagram, generally with higher crossing number.

We will devote the rest of the section to proving the following theorem.

**Theorem 6.2.1.** *Let  $L_1$  and  $L_2$  be links. Let  $D_1$  be a diagram of  $L_1 \cup U$  and  $D_{n+1}$  be a diagram representing  $L_2$ . Suppose  $D_1, \dots, D_{n+1}$  are a sequence of diagrams where  $D_i$  differs from  $D_{i+1}$  by isotopy and a single Reidemeister I or II move for  $i = 0, \dots, n-1$  and that  $D_n$  differs from  $D_{n+1}$  by a merge between a component of  $L_1$  and the added unknot. Then the induced chain map is an injection:*

$$\mathcal{H}^{i,j}(L_1) \hookrightarrow \mathcal{H}^{i,j}(L_2) \text{ for all } i, j$$

We start with the diagram  $D_0$ , which is a diagram from  $L_1$ . We can map into the chain complex for the diagram  $D_1$  using a map which is the identity on  $L_1$  and

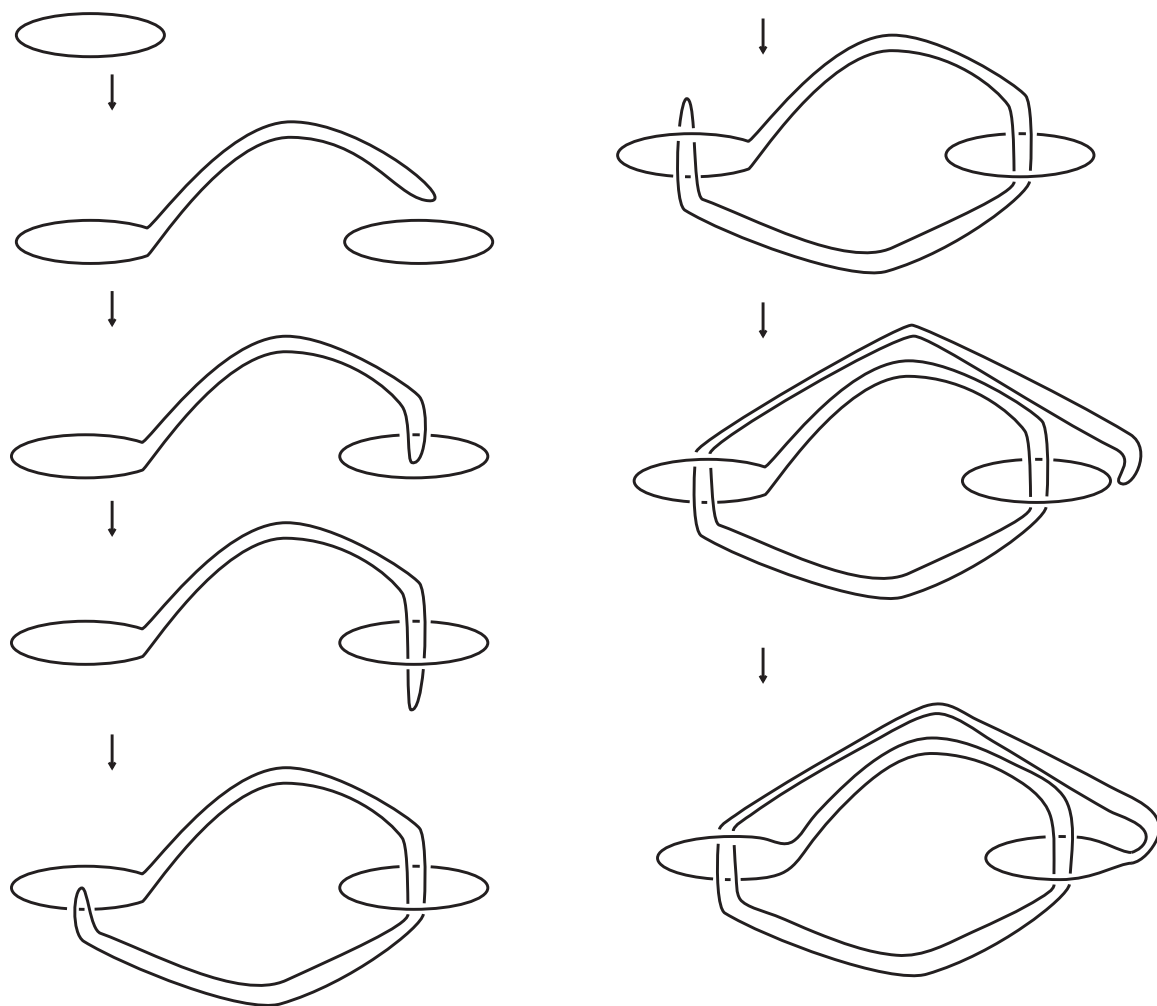


Figure 6.1: Constructing the  $6_1$  knot with ribbon moves

a birth to the unknot. Each subsequent diagram in the series  $D_1, \dots, D_{n+1}$  is gotten by performing a Reidemeister I or II move on the selected strand of  $L_1$ .

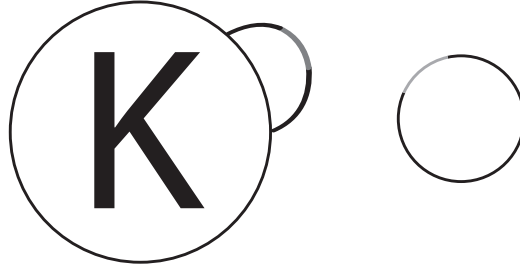


Figure 6.2: The diagram  $D_1$

We continue using the Reidemeister I and II moves until we reach diagram  $D_n$ . At each stage, we get a chain map  $f_i : C(D_i) \rightarrow C(D_{i+1})$  and a resulting composition from  $f_{0,n} : C(D_0) \rightarrow C(D_n)$ . The final move is to perform a merge between the chosen strand and a piece of the unknot. So we get a chain map from  $C(D_0) \rightarrow C(D_{n+1})$  which is determined by a birth, a series of Reidemeister moves, and finally a merge between link components. We show that this map is injective by providing an inverse map. The last operation performed in the composition was a merge between two link components. This means the first operation in the reverse process will split the two link components. As shown in the section 1 of this chapter, performing a merge and split in succession one obtains a neck which can be cut. The resulting map from  $C(D_n) \rightarrow C(D_n)$ , obtained by neck cutting, can be described by dotted diagrams, one dotted on the link component at the merge point, the other dotted on the unknot component. To construct the map back to the original chain complex, we simply undo all the Reidemeister moves in reverse order. We can perform inverse Reidemeister moves to get maps from  $C(D_{i+1})$  to  $C(D_i)$ . At each stage of the composition, either the Reidemeister involves a dotted strand and the dot will “carry” through the diagram, or the Reidemeister move occurs away from the dot and the dot remains on the map. The result of the total composition from  $C(D_0) \rightarrow C(D_0)$  will be a birth, Reidemeister moves, a neck cutting resulting in a pair of dotted maps, inverse Reidemeister moves, and finally a death. Below is a diagram representing the composition of the maps from  $C(D_1) \rightarrow C(D_1)$  before the birth and death occur.

One can see that the application of the initial birth and final death maps will result



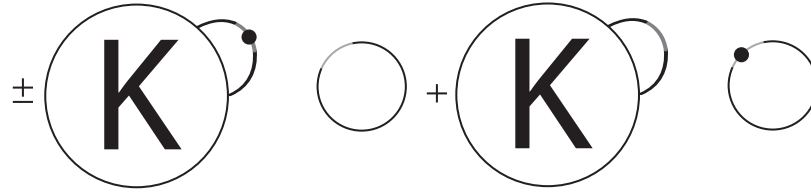


Figure 6.3: The resulting chain map  $C(D_1) \rightarrow C(D_1)$

in a sphere on the first term and a dotted sphere on the second. Given the relations in Khovanov homology, the map which contains a closed sphere will result in the 0 map. The second will be the identity map with a closed dotted sphere on  $C(D_0)$ . The dotted sphere can be removed and replaced with a coefficient of 1. All maps used in the process were chain maps, so we get that the  $\mathcal{H}(D_0)$  “factors through”  $\mathcal{H}(D_{n+1})$ . Thus the homology injects as desired.

### 6.3 Examples and Ribbon Knot Construction

A note about the limitations of this technique. The simplest application of this technique is equivalent to taking the connected sum with an unknot. The homology of the larger knot clearly injects in this case. The technique does not work for general connected sums, as we need to be able to “cap off” one of the links to get the desired identity on one of the components. Even if one of the components is slice (that is it bounds a locally flat disc in  $D^4$ ) the resulting induced map may not be injective on homology. The result can be applied in succession to obtain a chain of injecting homologies. For example, we have the following two stage construction of a ribbon knot where the ribbon moves attaching the new discs are highlighted.

The resulting injection of homologies is best observed by looking at the coefficients of the Poincarè polynomials of the corresponding knots. The terms in the second polynomial corresponding to terms in the first are highlighted. The Khovanov homology of the knot in the upper right portion of the diagram is given by:

$$\frac{2}{q} + q + \frac{1}{q^5 t^2} + \frac{1}{qt} + qt + q^3 t + q^5 t^2 + q^5 t^3 + q^9 t^4$$

and the homology of the knot in the lower half of the diagram is given by:

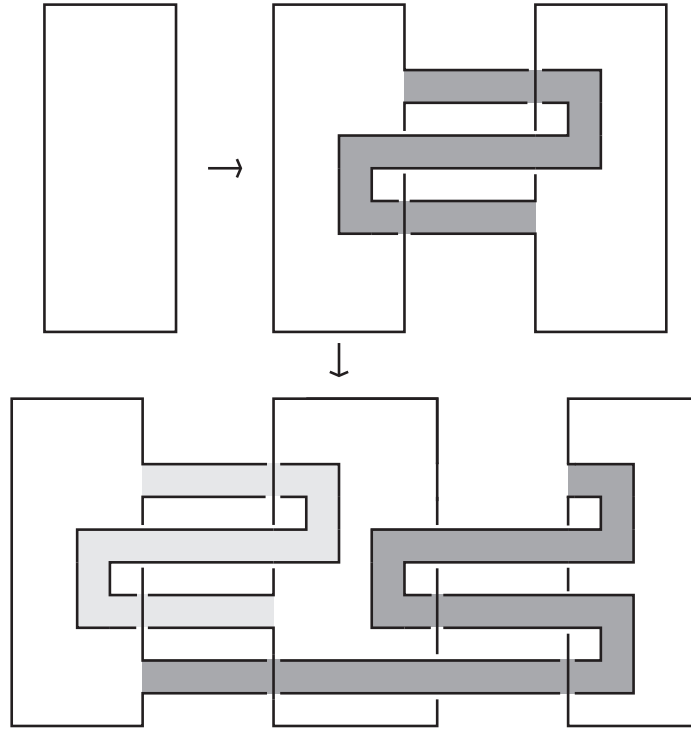


Figure 6.4: Two stage ribbon knot construction

$$\frac{4}{q} + 2q + \frac{1}{q^5 t^2} + \frac{1}{q^3 t} + \frac{1}{qt} + 4qt + 3q^3 t + 5q^3 t^2 + 4q^5 t^2 + 6q^5 t^3 + 5q^7 t^3 + 6q^7 t^4 + 6q^9 t^4 + \dots + q^{21} t^{10}$$

The homology of the knot indicates that it is not equivalent to a known ribbon knot with fewer than 12 crossings. We also have an example to show that this construction can be used to construct prime knots which are not ribbon. We show a ribbon move on a diagram of the trefoil to create the knot  $10_{147}$ . Again, the ribbon move used to attach the unknot is highlighted.

We show the homology of the trefoil :

$$q + q^3 + q^5 t^2 + q^9 t^3$$

injects into the homology of the knots  $10_{147}$ :

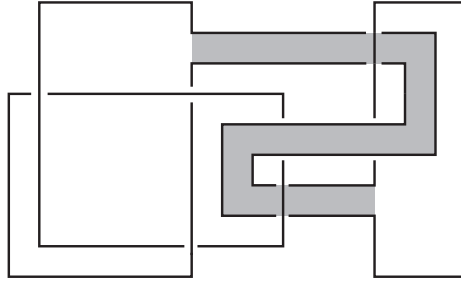


Figure 6.5: Construction of the knot  $10_{147}$  from the trefoil knot

$$\begin{aligned}
 3\mathbf{q} + 3\mathbf{q}^3 + \frac{1}{q^7 t^4} + \frac{1}{q^5 t^3} + \frac{1}{q^3 t^3} + \frac{2}{q^3 t^2} + \frac{1}{q t^2} + \frac{2}{q t} + \frac{2q}{t} + \\
 2q^3 t + 2q^5 t + 2\mathbf{q}^5 \mathbf{t}^2 + 2q^7 t^2 + q^7 t^3 + 2\mathbf{q}^9 \mathbf{t}^3 + q^{11} t^4
 \end{aligned}$$

One should also note that the injectivity result has no analog for the Jones polynomial, nor does the Jones polynomial indicate whether an injection is possible. Comparing the Jones polynomial of the trefoil

$$-\frac{1}{q^9} + \frac{1}{q^5} + \frac{1}{q^3} + \frac{1}{q}$$

to the Jones polynomial of the  $10_{147}$  knot,

$$\frac{1}{q^7} - \frac{1}{q^5} + \frac{1}{q^3} - \frac{1}{q} + q + q^3 + q^7 - 2q^9 + q^{11}$$

we can see that the exponents do not align. Moreover, the coefficients  $q^{-5}$  and  $q^{-1}$  differ in sign.

Another question one may ask is whether or not injection of homology is a rare occurrence. To determine if an injection is possible, one can compare the coefficients of the respective Poincarè polynomials of knots. As shown above, the construction can be used to construct prime knots from other knots. We ran a check to see how likely this occurrence is by comparing homologies of prime knots with low crossing number. Without regarding differing orientations, there are 802 prime knots with fewer than 12 crossings. A computer comparison of the ranks of the Khovanov homology of each of the prime knots with fewer than 12 crossings shows that injection is only possible about 7% of the time. This is not just injectivity of certain homological and quantum degrees, but the entire homology of the knot. This fact is meant to illustrate the

bigrading of the homology is quite a restriction when considering comparing homology groups.

The previous example shows that we can construct non-ribbon knots using this technique by starting with a non-ribbon knot. If we restrict ourselves to constructions starting with the unknot, one can ask which ribbon knots can be created using this method. Any knot created using this technique starting from the unknot will clearly be ribbon. In Kawachi's book [Kaw96], he presents a table which shows that every ribbon knot with fewer than 11 crossings can be obtained using this construction with only one iteration. We give a presentation of the ribbon knot  $10_{99}$  from that table to demonstrate this construction.

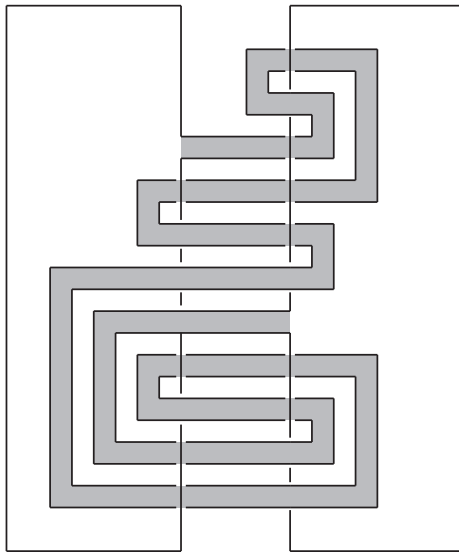


Figure 6.6: Construction of the knot  $10_{99}$

The next natural question is whether all ribbon knots can be created iteratively a single disk at a time. By definition, a ribbon knot  $K$  can be given by the boundary of a smooth disc in  $D^4$  such that  $\partial D = K$  and  $D$  admits no maxima. So, Morse theoretically, the disc bounding the ribbon knot will only have minima (which correspond to the addition of circles in our construction) and saddles. This leads to the following definition regarding the construction of ribbon disks. Let  $K$  be a ribbon knot in  $S^3$  and let  $D$  be a smooth disk in  $D^4$  with  $\partial D = K$  admitting no maxima. Let  $m(D)$  be the number of saddles in the given presentation of  $D$ .

**Definition 6.3.1.** Let  $K$  be a ribbon knot in  $S^3$ . The **saddle number** of  $K$ , denoted  $sn(K)$ , is given by

$$sn(K) = \min\{m(D) \mid D \text{ is a smooth disc in } D^4 \text{ with no maxima such that } \partial D = K\}$$

The diagrams in [Kaw96] show that  $sn(K) = 2$  for all ribbon knots with fewer than 11 crossings. We present a knot  $K$  in figure 6.7 with  $sn(K) \leq 2$ . The construction uses 3 discs and two saddles, which can not obviously be added in succession.

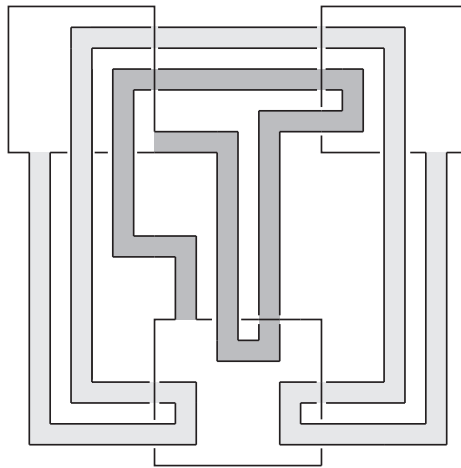


Figure 6.7: Construction of a ribbon knot using three minima and two saddles

Ribbon knots and ribbon cobordisms (cobordisms without maxima) form a category. Khovanov homology provides a functor from this category to the category of abelian groups. The maps induced by this construction are taken to injective maps under this functor. The construction is directional, but it is unclear whether the construction can “simplify” a knot. Showing that the functor applied to the surfaces made using this construction are actually proper injections would answer this question.

## 6.4 Future Work

The use of ribbon moves to construct knots and knot cobordisms leaves many directions for future work. One of the first questions to investigate is whether or not this construction can create a knot that has a lower crossing number. It is still an open question whether the crossing number is additive under connected sum [Lac09]. Using

the crossing numbers of the knots to determine their complexity would accomplish this goal. Another way to measure complexity is to compare the total ranks of the Khovanov homology of the knots (*i.e.* comparing  $Kh(K)(1,1)$  for each knot  $K$ ). Experimentally, the knots created using this technique always have higher total rank. For example,  $Kh(3_1)(1,1) = 4$  where  $Kh(10_{147})(1,1) = 28$ .

The difference in total rank also appears to be related directly to the complexity of the ribbon move. Twisting the ribbon using a Reidemeister I move experimentally results in a shift in homological degree, but the number of Reidemeister II moves used appears to increase the total rank. We present two ribbon knots in figure 6.8 both of which represent 10 crossing ribbon knots. The total homological rank of the two knots are  $Kh(10_3)(1,1) = 26$  and  $Kh(10_{35})(1,1) = 50$ . By comparison, the simplest such ribbon knot has total rank  $Kh(6_1)(1,1) = 10$ .

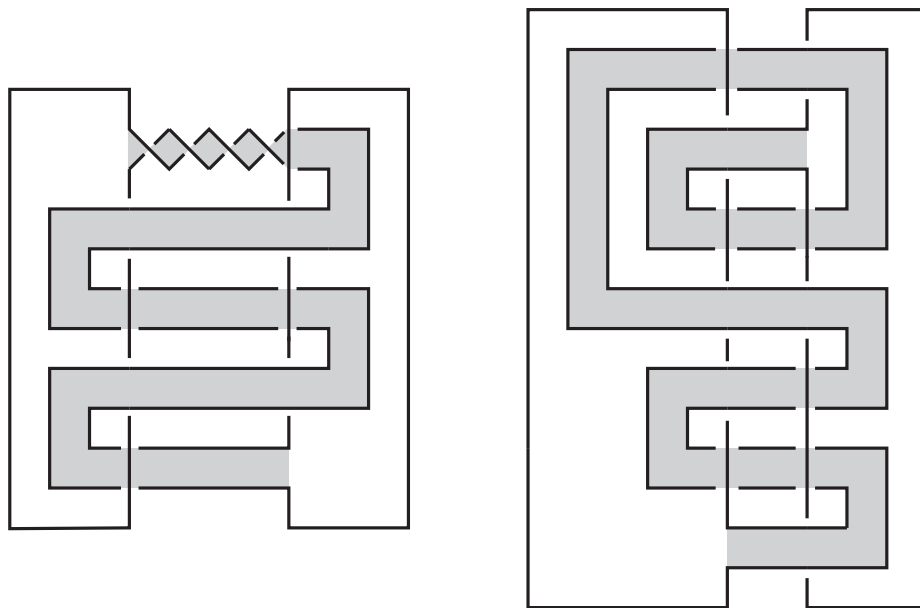


Figure 6.8: Ribbon presentations of the knots  $10_3$  and  $10_{35}$

The total rank of the homology appears to be more aligned with the complexity of the ribbon presentation rather than the crossing number of the knot. The Alexander polynomial is well known to encode strong topological properties. For example, the Alexander polynomial gives an upper bound for the 3-genus of a knot and the Fox-Milnor condition states that the Alexander polynomial of a ribbon or slice knot admits symmetric factorization. No such analog is known for the Jones polynomial or

Khovanov polynomial. The total rank of the Khovanov homology appears to pick up the complexity of the ribbon presentation of the knot. So, one can ask how surfaces bounding the knot affect the total rank of the homology. To illustrate this relationship further, we provide a table of the total ranks of the ribbon knots with fewer than 11 crossings along with a measure of the complexity of their ribbon presentations. We define  $\mathbf{rs}(\mathbf{D})$ , the ribbon number, of a ribbon diagram  $D$  to be the number of ribbon singularities in the diagram  $D$ . For example, the ribbon numbers of the diagrams in figure 6.8 are 4 and 6 respectively. We use the diagrams present in Kawauchi's book for the purpose of computing the ribbon number.

Table 6.1: Total ranks of ribbon knots of fewer than 11 crossings

Knot	Total Rank	$rs(D)$	Knot	Total Rank	$rs(D)$
$6_1$	10	2	$10_{48}$	50	6
$8_8$	26	4	$10_{75}$	82	8
$8_9$	26	4	$10_{87}$	82	8
$8_{20}$	10	2	$10_{99}$	82	8
$9_{27}$	50	6	$10_{123}$	122	10
$9_{41}$	50	6	$10_{129}$	26	4
$9_{46}$	10	2	$10_{137}$	26	4
$10_3$	26	4	$10_{140}$	10	2
$10_{22}$	50	6	$10_{153}$	18	3
$10_{35}$	50	6	$10_{155}$	26	4
$10_{42}$	82	8			

The table presents an interesting correspondence between the ribbon singularity number and the total rank. This is indicative of the Khovanov homology picking up information regarding bounding surfaces and their embeddings. The table also indicates a couple of patterns in the total rank of ribbon knots. First, a definition.

**Definition 6.4.1.** We say that knot  $K$  of **square rank** if  $Kh(K)(1, 1) = n^2 + 1$  for some integer  $n$ .

One will notice that many of the total ranks in the table are of the form  $(rs(D) + 1)^2 + 1$ . This does not hold for all ribbon knots. One can construct a ribbon knot  $D$

with  $rs(D) = 7$  and  $Kh(D)(1, 1) = 626 = 25^2 + 1$ . As we can see from the total rank of the ribbon knot  $10_{153}$ , not all of the ribbon knots are of square rank. One may ask how often knots are of square rank. Amongst prime knots with crossing number less than 12, square rank knots are rare. It is a known fact that for any knot  $K$ , the knot  $K\#mK$  is ribbon. Calculating the Khovanov homology for all knots of the form  $K\#mK$ , where  $K$  is prime and has fewer than 12 crossings, one sees that many of the total ranks are squares plus one. There are knots which are not ribbon but are of square rank. This identification does not give a criterion for being ribbon, but it is worth investigating why so many ribbon knots are of square rank, and so many non-ribbon knots are not.

Another observation is that for each ribbon knot  $K$  in the table,  $Kh(K)(1, 1) \cong 2 \pmod{8}$ . This does not hold for other knots. For example, the total rank of the trefoil knot is 4. The  $\pmod{8}$  congruence of the total rank was verified for all knots  $K\#mK$  where  $K$  is a prime knot with fewer than 12 crossings. Notice also that  $Kh(3_1)(1, 1) \cong Kh(10_{147})(1, 1) \pmod{8}$  and the two are related via a ribbon move. This observation leads us to the following conjectures.

**Conjecture 6.4.2.** *If  $K$  is a ribbon knot, then*

$$Kh(K)(1, 1) \cong 2 \pmod{8}$$

The ribbon construction is an example of a concordance between knots. One may also make the following conjecture.

**Conjecture 6.4.3.** *If  $K_1$  is concordant to  $K_2$ , then*

$$Kh(K_1)(1, 1) \cong Kh(K_2)(1, 1) \pmod{8}$$

The phenomenology discussed in this section is quite surprising. If these techniques or observations can be used to find a criterion for ribbon knots, Khovanov homology will become a better tool for studying the potential gap between ribbon and slice knots. The empirical evidence that Khovanov homology is detecting the complexity of smooth bounding surfaces of knots is worthy of further study.



# Bibliography

- [Abe10] Tetsuya Abe. The Rasmussen invariant of a homogeneous knot. *arXiv:1003.5392v1 [math.GT]*, 2010.
- [BN05] Dror Bar-Natan. Khovanov's homology for tangles and cobordisms. *Geometry and Topology*, 2005.
- [BN07] Dror Bar-Natan. Fast Khovanov homology computations. *J. Knot Theory Ramifications*, 2007.
- [CMW09] David Clark, Scott Morrison, and Kevin Walker. Fixing the functoriality of Khovanov homology. *Geom. Topol.* 13, 2009.
- [Jac04] Magnus Jacobsson. An invariant of link cobordisms from Khovanov homology. *Geometric Topology*, 2004.
- [Kaw96] Akio Kawauchi. *A Survey of Knot Theory*. Birkhäuser, 1996.
- [Kho00] Mikhail Khovanov. A categorification of the Jones polynomial. *Duke Math. J.*, 2000.
- [Kho03] Mikhail Khovanov. Patterns in knot cohomology, I. *Experimental Mathematics*, 2003.
- [Lac09] Marc Lackenby. The crossing number of composite knots. *J. Topology*, 2009.
- [Lee02] Eun Soo Lee. The support of the Khovanov's invariants for alternating knots. *arXiv:math/0201105*, 2002.
- [MBN] Scott Morrison and Dror Bar-Natan. The knot atlas. <http://katlas.org>.
- [Ras04] Jacob Rasmussen. Khovanov homology and the slice genus. *Geometry and Topology*, 2004.
- [Sto07] Marko Stosic. Homological thickness and stability of torus knots. *Algebraic and Geometric Topology*, 2007.
- [Sul97] Michael Sullivan. Positive braids with a half twist are prime. *Journal of Knot Theory and Its Ramifications*, 1997.